

1 **Isohydricity and hydraulic isolation explain**
2 **reduced hydraulic failure risk in an**
3 **experimental tree species mixture**

4
5 Myriam Moreno ^{1,2, *}, Guillaume Simioni ¹, Hervé Cochard ³, Claude Doussan ⁴,
6 Joannès Guillemot ^{5,6,7}, Renaud Decarsin ¹, Pilar Fernandez-Conradi ¹, Jean-Luc
7 Dupuy ¹, Santiago Trueba ⁸, François Pimont ¹, Julien Ruffault ¹, Frederic Jean ¹,
8 Olivier Marloie ¹, and Nicolas K. Martin-StPaul ¹

9
10
11 ¹ URFM, INRAE, 84914 Avignon, France

12 ² French Environment and Energy Management Agency, 49000 Angers, France

13 ³ PIAF, INRAE, Université Clermont Auvergne, 63000 Clermont-Ferrand, France

14 ⁴ EMMAH, INRAE, 84914 Avignon, France

15 ⁵ UMR Eco&Sols, CIRAD, 34398 Montpellier, France

16 ⁶ Eco&Sols, Univ Montpellier, CIRAD, INRAE, IRD, Montpellier SupAgro, 34398
17 Montpellier, France

18 ⁷ Department of Forest Sciences, ESALQ, University of São Paulo, Piracicaba, São
19 Paulo, Brazil

20 ⁸ BIOGECO, INRAE, Université de Bordeaux, 33615 Pessac, France

21
22
23 * Myriam Moreno (corresponding author).

24 **Email:** myriam.moreno@inrae.fr

25
26
27
28
29
30 The author responsible for distribution of materials integral to the findings presented
31 in this article in accordance with the policy described in the Instructions for Authors
32 (<https://academic.oup.com/plphys/pages/General-Instructions>) is Myriam Moreno.

36 Abstract

37 Species mixture is promoted as a crucial management option to adapt forests to
 38 climate change. However, there is little consensus on how tree diversity affects tree
 39 water stress, and the underlying mechanisms remain elusive. By using a greenhouse
 40 experiment and a soil-plant-atmosphere hydraulic model, we explored whether and
 41 why mixing the isohydric Aleppo pine (*Pinus halepensis*, drought avoidant) and the
 42 anisohydric holm oak (*Quercus ilex*, drought tolerant) affects tree water stress during
 43 extreme drought. Our experiment showed that the intimate mixture strongly alleviated
 44 *Q. ilex* water stress while it marginally impacted *P. halepensis* water stress. Three
 45 mechanistic explanations for this pattern are supported by our modelling analysis.
 46 First, the difference in stomatal regulation between species allowed *Q. ilex* trees to
 47 benefit from additional soil water in mixture, thereby maintaining higher water
 48 potentials and sustaining gas exchange. By contrast, *P. halepensis* exhibited earlier
 49 water stress and stomatal regulation. Second, *P. halepensis* trees showed stable water
 50 potential during drought, although soil water potential strongly decreased, even when
 51 grown in a mixture. Model simulations suggested that hydraulic isolation of the root
 52 from the soil associated with decreased leaf cuticular conductance was a plausible
 53 explanation for this pattern. Third, the higher predawn water potentials for a given
 54 soil water potential observed for *Q. ilex* in mixture can - according to model
 55 simulations - be explained by increased soil-to-root conductance, resulting from
 56 higher fine root length. This study brings insights into the mechanisms involved in
 57 improved drought resistance of mixed species forests.

58

59

60

61 Keywords

62 Forest, functional diversity, drought resistance, tree hydraulic, safety margins.

63

64 Introduction

65

66 The rising frequency and intensity of extreme droughts is impacting tree survival and
 67 forest functions worldwide (Allen et al., 2010; Breshears et al., 2013; Senf et al.,
 68 2020), jeopardizing crucial forest ecosystem services. Tree species diversity has been
 69 promoted as an important nature-based solution to improve the resilience of forests
 70 and tree plantations (Messier et al., 2022). The effects of species mixing on drought
 71 resistance could result from different mechanisms, such as competitive reduction for
 72 water through resource partitioning or facilitation – for instance hydraulic
 73 redistribution (Grossiord, 2020). Yet, tree species diversity effect on tree drought
 74 resistance are not universal and can change in direction and magnitude according to
 75 the sites, the species of the composition of the mixture (Grossiord, 2020; Grossiord et
 76 al., 2014b; Mas et al., 2024). Indeed, previous studies showed that tree species
 77 diversity effect can have positive (de-Dios-García et al., 2015; Lebourgeois et al.,
 78 2013; Ruiz-Benito et al., 2017), neutral (Grossiord et al., 2014b; Merlin et al., 2015)
 79 or even negative impacts (Grossiord et al., 2014a; Vitali et al., 2018). These
 80 conflicting results suggest that it is not the species richness that matters, but rather the
 81 functional composition of the mixtures (i.e., the association of species with different
 82 drought response strategies) (Forrester and Bausch, 2016; Grossiord, 2020). This

83 hypothesis was supported by recent research that found that the diversity of hydraulic
 84 traits determines the resilience to drought of forest water fluxes globally (Anderegg et
 85 al., 2018). Similarly, results from a large-scale tree diversity experiment showed that
 86 the diversity of drought resistance strategies is a good predictor of the stability of tree
 87 growth and forest productivity (Schnabel et al., 2021). However, we crucially miss a
 88 mechanistic understanding of the way the diversity of drought resistance strategies
 89 mediates tree mortality under extreme drought.

90 Tree species drought resistance strategies result from a set of functional traits that
 91 determine how rapidly plant water status (often quantified as water potential) crosses
 92 vital physiological thresholds. In particular, drought resistance strategies determine
 93 the loss of hydraulic conductance caused by a high rate of embolism in xylem
 94 conduits (Tyree and Sperry, 1989), i.e., the risk of xylem hydraulic failure, a leading
 95 mechanism in drought-induced tree mortality (Adams et al., 2017; Sanchez-Martinez
 96 et al., 2023).

97 It is common in the literature to distinguish species drought resistance strategies based
 98 on the water loss regulation through stomatal closure (Klein, 2014; Martin-StPaul et
 99 al., 2017) - and the xylem vulnerability to embolism (Choat et al., 2018; Delzon,
 100 2015; Martin-StPaul et al., 2017). Isohydic species (sometime also referred as
 101 drought avoidant) close their stomata relatively early during drought and have a lower
 102 cuticular conductance. Therefore, they limit soil water depletion, which in turn limits
 103 the soil and plant water potential decrease and the overall risk of hydraulic failure
 104 (Delzon, 2015; López et al., 2021). They also tend to have relatively narrow safety
 105 margins, and are less embolism-resistant than anisohydric species. Anisohydric
 106 species (also referred as drought tolerant), have higher resistance to drought-induced
 107 xylem embolism. However, they tend to maintain gas exchanges during drought via a
 108 delayed stomatal regulation and relatively higher cuticular conductance. This implies
 109 greater soil water depletion and greater drop in soil and plant water potential during
 110 drought (Choat et al., 2018; Martin-StPaul et al., 2017) (Figure 1A).

111 Based on this knowledge, one can hypothesize how mixing two species with such
 112 distinct drought response strategies will impact soil water dynamic, plant water status
 113 (water potentials), and the risk of hydraulic failure under extreme drought. To
 114 facilitate the reasoning, we assume that trees are hydraulically connected to the soil
 115 (*i.e.*, soil and plant predawn water potential are very close) and that the root systems
 116 of both species are intimately mixed and fully occupy a given soil volume. We can
 117 then derive three complementary hypotheses (which are also depicted on Figure 1B):

118 **(1)** For an anisohydric (drought tolerant) species, it is beneficial to compete for water
 119 with an isohydric (drought avoidant) neighbour. Indeed, the soil water saved by
 120 earlier stomatal regulation of the isohydric is available to maintain gas exchanges and
 121 delay the decrease in water potential and the overall hydraulic failure risk (Figure 1B).

122 **(2)** By contrast, mixing is detrimental to an isohydric (isohydric) species, as it
 123 experiences lower soil water potential due to sustained water-use by the companion
 124 anisohydric species. This leads to a decrease in its water potential, thereby increasing
 125 the risk of hydraulic failure. The scenario presented in Figure 1B - which shows that
 126 an anisohydric always “wins the fight” during drought under mixture - holds only if
 127 the predawn water potential of the mixed species is at equilibrium with the soil water
 128 potential.

129 (3) If the root systems of the two neighbour species are segregated in space, water
 130 consumption by the anisohydric species does not affect the isohydric species, and
 131 differences in water potentials between tree species in the mixture could occur given
 132 their spatial isolation (Figure 1B). In support to this hypothesis, root niche separation
 133 is often proposed as a mechanism allowing to reduce water stress for trees associated
 134 in mixture (Grossiord, 2020; Jose et al., 2006).

135 In this study, we combined a greenhouse experiment and a mechanistic model
 136 analysis to evaluate these hypotheses and explore the mechanisms and traits involved
 137 in the modulation of water stress in mixed forests during an extreme drought. We
 138 compared the ecophysiological responses to drought of holm oak (*Quercus ilex*) and
 139 Aleppo Pine (*Pinus halepensis*) grown in monocultures and in mixtures. In order to
 140 evaluate the importance of having root systems intimately mixed, we also added a
 141 treatment in which the root systems of the two plants were separated (Figure 1B).

142

143 Results

144 a) Water status dynamic in the different treatments

145 Soil water content, soil water potential (Ψ_{soil}) and plant predawn water potential (Ψ_{pd})
 146 declined during drought for both species and in all pot compositions (Figures 2A and
 147 Figures S1). In accordance, soil electrical resistivity increased during drought (Figure
 148 S2). However, the temporal dynamics differed between species, in agreement with
 149 their drought-response strategies (Moreno et al., 2021). Ψ_{pd} decline was more
 150 pronounced for the anisohydric *Q. ilex*, which exhibited Ψ_{pd} as low as -8 MPa, than
 151 for the isohydric *P. halepensis*, for which Ψ_{pd} did not go below -4 MPa regardless of
 152 the pot composition (Figure 2A, Table S1 with P-value < 0.001 for the species effect).
 153 Gas exchanges also decreased for the two species (Figure S3 P-value > 0.05) for all
 154 pot compositions, but the decrease tended to occur earlier for the isohydric *P.*
 155 *halepensis* than for the anisohydric *Q. ilex* (Figure S3).

156

157 For *Q. ilex*, our empirical data suggested a positive effect of mixture (without
 158 separation) on drought stress at the early stage of drought as leaf gas exchanges
 159 tended to be slightly higher in mixture than in monoculture at the second date of
 160 measurements (Figure S3). This trend was confirmed during extreme drought (latest
 161 date of the experiment) on plant water potential (Figure 2A), which was significantly
 162 higher in mixture than in monoculture (mean Ψ_{pd} of -6.37 MPa in mixture against
 163 mean Ψ_{pd} of -8.3 MPa in monoculture; Table S2 P-value < 0.01 for the date:mixture
 164 interaction effect). At the drought peak, this water potential difference between
 165 treatments translated into a significant effect on hydraulic safety margins (mean HSM
 166 = $\Psi_{\text{pd}} - P50$, an indicator of the risk of hydraulic failure), which was higher in mixture
 167 (mean HSM = 0.73 MPa) than in monoculture (mean HSM = -1.33 MPa) for *Q. ilex*
 168 (Figure 2B, P-value < 0.05). For *P. halepensis*, there was also a trend toward lower
 169 gas exchange in mixture during early drought (Figure S3). However, during extreme
 170 drought, we found no significant difference in plant water potential (Table S2, P-value
 171 > 0.05 for the date:mixture interaction effect) and thus HSM (Figure 2B, P-value >
 172 0.05) was found between treatments (Mean HSM = 1.1 MPa in mixture and 1.43 MPa
 173 in monoculture).

174

175 For both species, plants grown in mixture with a root separation treatment exhibited
 176 no significant difference with monoculture for gas exchange or plant water potential.

177 This indicates that mixture only had an effect on water stress if tree root systems were
 178 intimately entangled. This result was supported by an analysis showing that water
 179 flow from one compartment to the other of the pot equipped with a mesh (i.e., through
 180 the mesh) during drought is very limited (Supplemental Method S1 and Table S3). In
 181 brief, we applied Darcy's law for different types of soil textures using water potential
 182 gradient as the difference in predawn water potential between the two species at the
 183 penultimate and last dates of measurements (largest water potential gradient measured
 184 for the experiment). We found that water flow occurring between the two plant
 185 species through the mesh was very low, and negligible compared to the transpiration
 186 flow, due to the very sharp decline in soil hydraulic conductivity.

188 **b) Modification of the plant vs. soil water potential relationship in mixture**

189 During the beginning of the drought, Ψ_{pd} and Ψ_{soil} were very close for both species
 190 (Figures 2A, 3A) in all treatments. However, as drought gradually increased Ψ_{pd} and
 191 Ψ_{soil} differed progressively for both species and in all treatments except for *Q. ilex* in
 192 mixture (Figures 2A, 3A). The slope of the Ψ_{pd} vs Ψ_{soil} relationship differed between
 193 species (Figure 3A). Whereas Ψ_{pd} became lower than Ψ_{soil} for *Q. ilex* with increasing
 194 drought, Ψ_{pd} became higher than Ψ_{soil} for *P. halepensis*. Such observation remained
 195 significant even when considering the uncertainty in calculating Ψ_{soil} (Figure S4). The
 196 fact that Ψ_{soil} was more negative than Ψ_{pd} for *P. halepensis* in the monoculture
 197 suggests that some soil evaporation occurred, due to imperfect covering of the pots or
 198 to the holes made in the pots for the drainage of water and the measurement of soil
 199 resistivity. A peculiar pattern was found for *Q. ilex* in mixtures (without root
 200 separation), for which Ψ_{pd} equalled Ψ_{soil} all along the desiccation dynamic (Figure 3A;
 201 Table 1, P-value = 2.12e-07 for the Ψ_{soil} : Pot modalities effect). Indeed, the slope of
 202 the relationship between Ψ_{pd} and Ψ_{soil} for *Q. ilex* in mixtures without root separation
 203 was close to 1, but was 1.74 for the other pot modalities (Table 2, P-value < 0.001 for
 204 the Ψ_{soil} : Mixture without root sep. interaction).

206 Changes in the behaviour of *Q. ilex* in mixture was further confirmed by exploring the
 207 relationship between the Ψ_{pd} of the two species in mixtures with and without root
 208 separation (Figure 3A). We found a significantly lower slope (slope = 1.6) in the
 209 mixture without root separation than in the mixture with root separation (slope = 2.21;
 210 Figure 3B, Table 3, P-value = 0.03 for the species x separation modality interaction).

212 **c) Results of the model simulations and sensitivity analysis**

213 The Figure 4 shows simulation results with the SurEau model for water potential and
 214 transpiration under "benchmark" conditions (i.e., traits were set according to the
 215 hypothesis formulated in Figure 1B). In these simulations, the anisohydric (*Q. ilex*)
 216 exhibited an increase in transpiration by 20% and experienced a later time to hydraulic
 217 failure (THF) (increased by a factor of 1.5) in mixture compared to monoculture. On
 218 the contrary, the isohydric species (*P. halepensis*) showed a reduction of transpiration
 219 by ca. 20% and an earlier THF twice shorter in mixture than in monoculture. In
 220 addition, Ψ_{pd} (maximal daily Ψ_{plant} , taken at night) and Ψ_{soil} were always very close to
 221 each other until significant loss of plant hydraulic conductance occurred.

222 These simulations were consistent with the hypotheses drawn in Figure 1B, but not
 223 with the experimental results (Figure 2). Simulations departed from our empirical
 224 findings on two points. Simulations showed (1) greater water stress for *P. halepensis*
 225 in mixture and (2) a tight relationship between Ψ_{pd} and Ψ_{soil} , for the two species.

226 We conducted different sensitivity analyses (Figure 5) to further understand the
227 reasons underpinning the departure between model and experimental data.

228 First, we tested if plant isolation (i.e. “hydraulic decoupling”) could match the
229 empirical data (i.e., higher Ψ_{pd} than Ψ_{soil}) during drought for the isohydric *P.*
230 *halepensis*. We first implemented a root to soil hydraulic isolation by applying a
231 decrease in root hydraulic conductance (K_{root}) as Ψ_{plant} decline (Figure S5). This did
232 not allow to simulate higher Ψ_{pd} than Ψ_{soil} for this species (Figure 5A, variable K_{root}).
233 Second, we implemented a leaf to air hydraulic isolation by implementing a decrease
234 of the leaf cuticular conductance (g_{cuti}) (i.e., isolation from air dryness, Figure S6 A)
235 with decreasing leaf relative water content, in accordance with empirical data
236 obtained in *P. halepensis* using the drought-box method (Billon et al., 2020) (Figure
237 S6 B). The results showed that reducing only g_{cuti} did not allow to match the empirical
238 pattern ($\Psi_{pd} > \Psi_{soil}$, Figure 5A, variable g_{cuti}). In a third simulation, we implemented
239 both a decrease of K_{root} and a decrease of g_{cuti} during drought stress. This allowed to
240 simulate a greater survival in mixture than in monoculture (similar THF), and $\Psi_{pd} >$
241 Ψ_{soil} in accordance with empirical results (Figure 5A, variables K_{root} and g_{cuti}). These
242 tests support that hydraulic isolation can be a way for Pine to maintain a constant
243 hydraulic risk during increasing drought even in mixture with and anisohydric oak.

244 Secondly, to explain the change in the Ψ_{pd} to Ψ_{soil} relationship observed for *Q. ilex* in
245 our empirical data (Figure 3A; Table 1, P-value = 2.12e-07 for the Ψ_{soil} : Pot
246 modalities effect), we tested the hypothesis of an enhanced soil hydraulic conductance
247 in mixture, through increased fine root length (equations 3 and 4 in M&M section).
248 This would be consistent with the observation of greater root length in mixture
249 (Figure S7). Simulation results showed that increasing soil hydraulic conductance
250 allowed Ψ_{plant} to keep closer to Ψ_{soil} during drought (Figure 5B).

251

252 Discussion

253

254 It has been hypothesized that competition for water during drought is reduced
 255 between species with contrasting hydraulic strategies (iso vs anisohydric) in mixtures
 256 (Anderegg et al., 2018; Bello et al., 2019; Haberstroh and Werner, 2022; Schnabel et
 257 al., 2021). However, very little is known about how species interactions affect tree
 258 resistance to extreme drought (Grossiord, 2020; Haberstroh and Werner, 2022) and
 259 experimental test comparing monocultures and mixtures of species with contrasting
 260 hydraulic strategies during extreme drought are lacking. The extreme drought
 261 experiment that we conducted in a greenhouse highlighted that mixing an isohydric
 262 and an anisohydric species strongly alleviated the water stress of the anisohydric
 263 species, while it had a relatively weak impact on the water stress of the isohydric
 264 species (Figure 2). This result is only partially in agreement with the initial
 265 hypotheses drawn in Figure 1B, and with the benchmark model simulations that were
 266 based on these hypotheses (Figure 4). Our data and model analyses helped to identify
 267 three mechanistic explanations for these results: (i) the differences in water use
 268 strategy between the two species, (ii) the ability of *P. halepensis* to isolate (or
 269 disconnect) during drought and (iii) the changes in the soil hydraulic conductance
 270 possibly related to fine root density. These mechanisms are discussed in the
 271 following.

272

273 a) Differences in water use strategy partly explain the mixture effect on gas 274 exchanges and hydraulic risk

275

276 Experimental data supported that *Q. ilex* could maintain gas exchange longer and
 277 experienced lower hydraulic risk during drought in the “true mixture” (i.e., pots
 278 designed without root separation) than in the monoculture (Figure 2, S3). This pattern
 279 is in agreement with our initial hypothesis H1 (Figure 1B) and with previous
 280 assumptions of the literature (Bello et al., 2019; Mas et al., 2024). In addition, such
 281 empirical results were confirmed by the SurEau simulations under benchmark
 282 conditions that were fully in line with our initial hypothesis (Figure 4). For *P.*
 283 *halepensis*, lower gas exchanges during early drought were measured in the “true
 284 mixture” than in the monoculture. This is also consistent with our initial assumption
 285 and with SurEau model simulations under benchmark conditions. The most
 286 straightforward explanation for these results, is the difference in stomatal behaviour
 287 between the two species, that has been proposed in the introduction: during drought, it
 288 is beneficial for an anisohydric species (such as *Q. ilex*) to compete with an isohydric
 289 (such as *P. halepensis*), because the earlier stomatal regulation of the isohydric save
 290 some water which is made available to the *Q. ilex* to maintain gas exchanges and
 291 delay the decrease in water potential and the overall hydraulic failure risk. On the
 292 contrary, for the isohydric species, being in mixture with an anisohydric would trigger
 an earlier drought stress and water losses regulation.

293

294 However, different experimental results departed from the initial assumptions and
 295 from the SurEau simulations under benchmark conditions, suggesting that additional
 296 effects were at play in the interspecific interaction. Firstly, for *Pinus halepensis*, no
 297 difference in predawn water potential between monoculture and mixture were found
 298 during extreme drought. And more importantly this species was able to maintain a
 299 predawn water potential higher than the soil water potential as commonly found in the
 300 field (e.g. Moreno et al 2021), which suggests that this species can limit its
 desiccation and maintain water status through some form of hydraulic disconnection.

301 For *Quercus ilex*, we found a change in the relationship between predawn water
 302 potential and soil water potential in mixture compared to monoculture (Figure 3),
 303 supporting that this species can maintain higher predawn water potential for a given
 304 level of soil drought in mixture. This is discussed in the third section of this
 305 discussion.

306

307 **b) Hydraulic disconnection (“isolation hypothesis”) of the isohydric *P.***
 308 ***halepensis* as a mean to limit hydraulic risk in mixture during drought**

309 The fact that *P. halepensis* exhibited higher Ψ_{pd} than Ψ_{soil} during drought when grown
 310 in mixture with *Q. ilex* (Figure 2) contradict our initial hypothesis (Figure 1B) and the
 311 model simulations under benchmark conditions (Figure 4). An explanation for this is
 312 the ability of this species to (i) disconnect (or isolate) from the soil (i.e., reducing the
 313 soil to tree hydraulic conductance) and (ii) limit its water losses during drought.
 314 Pioneering work on this topic were conducted by (Nobel and Sanderson, 1984) who
 315 showed that roots of desert succulent plants could act as “rectifier”, thereby being able
 316 to absorb water in wet soil, but to limit desiccation in dry soils, which seems
 317 consistent with our results.

318 We used the SurEau model to evaluate whether root hydraulic isolation from the soil
 319 could explain the observed water potential patterns in *P. halepensis* in mixture,
 320 consistently with (Nobel and Sanderson, 1984) work. We implemented a decrease in
 321 root hydraulic conductance (K_{root}) as the plant water potential decreases. Simulations
 322 results indicated that reducing only K_{root} alone did not allow to simulate higher Ψ_{pd}
 323 than Ψ_{soil} for *P. halepensis* (Figure 5A). This means that the water losses that occurred
 324 after stomatal closure – which resulted from the leaf cuticular conductance (g_{cuti}), set
 325 in the model using the average value measured for *P. halepensis*, was high enough to
 326 cause plant water potential to drop even after a strong decrease in K_{root} isolating the
 327 plant from the soil. We thus implemented in the model a down-regulation of the leaf
 328 cuticular conductance (g_{cuti}) with decreasing tree relative water content, which is in
 329 line with empirical data obtained for this species using the drought-box methods
 330 (Billon et al., 2020) (Figure S6 B). Simulations showed that, although the reduction of
 331 g_{cuti} alone attenuated the decrease in plant water potentials, the tree kept dehydrating
 332 along with the soil water potential drop triggered by *Q. ilex* transpiration. In a last
 333 sensitivity test, we implemented a decrease of both K_{root} and g_{cuti} under drought,
 334 which caused *P. halepensis* water potentials to depart from soil water potentials
 335 (Figure 5A), in line with our observations. This suggests that these two mechanisms
 336 jointly could allow *P. halepensis* to prevent dehydration under drought. In a natural
 337 forest context, tree isolation from the soil during drought has already been proposed to
 338 explain the co-occurrence of isohydric and anisohydric trees (Aguadé et al., 2015;
 339 Moreno et al., 2021; Pangle et al., 2012; Plaut et al., 2012). The mechanisms for such
 340 an isolation are of several types, including the formation of cortical lacunae under fine
 341 roots (Cuneo et al., 2016; Duddek et al., 2022), which reduces the water transfer to the
 342 root stele and hence affects the root hydraulic conductance. Root shrinkage might also
 343 explain the plant-soil hydraulic disconnection by creating gaps between soil and fine
 344 roots, interrupting the hydraulic conductance between both them. Furthermore, the
 345 inhibition of the synthesis of proteins such as aquaporins facilitating the water
 346 transport in the transcellular pathway (Domec et al., 2021), or even fine root mortality
 347 (Leonova et al., 2022) could also lead to hydraulic isolation. Yet, to our knowledge,
 348 the mechanisms leading to strong plant hydraulic isolation from both the soil and the
 349 atmosphere had never been proposed until now.

350 **c) The anisohydric *Q. ilex* could increase root hydraulic conductance to the**
 351 **soil in the mixture through increased root length**

352 *Q. ilex* in "true mixture" (i.e., pots without root separation), had lower water stress for
 353 a given level of soil drought (i.e., higher predawn water potential for a given soil
 354 water potential, Figure 3A). This suggests that this species is able to increase soil
 355 water use when grown in association with *P. halepensis*. Different hypothesis could
 356 explain this phenomenon. It could be argued that differences between Ψ_{pd} and Ψ_{soil}
 357 reflect shifts in the root profiles in mixtures compared to monocultures as proposed by
 358 (Bello et al., 2019). Indeed, if roots explored only a part of the available soil, Ψ_{pd}
 359 would equilibrate with this soil subspace, possibly differing from the overall Ψ_{soil}
 360 measured at the plot level. However, such an effect should be minimal in our study
 361 for two reasons. Firstly, we used on purposes very small pots (12 L) to maximize the
 362 occupation of the soil volume by tree roots, which was verified when the plants were
 363 uprooted at the end of the experiment, and thus makes this assumption unlikely.
 364 Secondly, the measurements of soil resistivity made at two different depths, showed
 365 no significant differences between the two measured depth levels (1/3 and 2/3 of the
 366 pot height), for none of the modalities (Figure S2, P-value > 0.05). Because resistivity
 367 varies according to a power law as a function of water content (Archie, 1942;
 368 Waxman and Smits, 1968), which means that when the soil is dry, little variation of
 369 soil water content translates into a large change in resistivity, our measurements
 370 indicate that there is most likely no spatial segregation in the uptake of soil water by
 371 roots. Alternatively, one can postulate that differences between Ψ_{pd} and Ψ_{soil} resulted
 372 from changes in the soil hydraulic conductance between, which could occur as a result
 373 of increase fine root density. We carried out simulations with SurEau to test this
 374 hypothesis (Figure 5B). Hence, we conducted simulations in which we assumed that
 375 the increase in soil conductance might be achieved through an increase in the
 376 exchange surface between soil and roots ("single root" approach, see materials &
 377 methods section). We tested this hypothesis by varying the fine root length per unit
 378 soil volume. This sensitivity test showed that changing K_{soil} can change the Ψ_{pd} vs
 379 Ψ_{soil} relationship (Figure 5B). Indeed, reducing the value of this parameter (graph
 380 "root length x 1/2", Figure 5B) resulted in a departure between Ψ_{pd} and Ψ_{soil} as
 381 observed in the monoculture, whereas increasing root length resulted in Ψ_{pd} and Ψ_{soil}
 382 being comparable, as observed in the mixture without root separation. Interestingly,
 383 some studies have already reported modifications toward higher fine roots density in
 384 mixture conditions (Sun et al., 2017; Wambsganss et al., 2021), identifying this
 385 phenomenon as a complementarity effect between associated species.

386 **d) Ecological and practical implications**

387 Our study has different larger scale implications for forest management and
 388 vegetation modelling. First of all, it is noteworthy that the positive effect of mixture --
 389 particularly highlighted for *Q. ilex* -- was not found in the pots designed to separate
 390 the root systems of the two species with a mesh (Figures 2, 3 and Figure S3). This
 391 indicates that root systems of the two individuals must be entangled for the mixture
 392 effect to be efficient. This result is important for tree plantation as it supports the
 393 premise that intimate species mixture is required to observe a mixture effect in diverse
 394 forests. Overall, this is in line with the growing body of evidence showing the
 395 importance of tree-tree interactions in driving the biodiversity vs ecosystem
 396 functioning relationships (Trogisch et al., 2021).

397 In addition, our study could explain how mixing tree species with contrasting
 398 hydraulic strategies limited the hydraulic risk during extreme drought by using a

399 mechanistic model. This paves the way for developing numerical tools allowing to
400 explore how to design species mixture resilient to climate change. Although the
401 mechanisms highlighted remain to be tested at larger scale, they could change our
402 representation of the mechanisms that determine water stress in plant communities.
403 Although positive effects of mixtures can come from a complementarity of water use
404 linked to spatial segregation of root systems or different water uptake depth as usually
405 propose (Bello et al., 2019; Grossiord et al., 2019; Haberstroh and Werner, 2022; Liu
406 et al., 2023) , we provided support that other mechanisms can be involved. Indeed,
407 differences in water use regulation strategies of species along with modifications of
408 hydraulic connections between the plant and the soil can alone explain the observed
409 behaviours in a model. This challenges the way vegetation models represent water
410 stress in plant communities. To date, the majority of process-based models assume
411 that soil water deficit in the rooting zone drives the water status of the plant.
412 However, we provide evidence that changes in the hydraulic connection from the soil
413 can make the plant, in dry conditions, behave independently from the soil water
414 status. Implementing such processes in larger scale vegetation models could help to
415 refine and better predict species interactions and drought induced effects on forest
416 communities. This would represent a step forward in the development of tools
417 allowing to design drought resilient mixtures.

418

419 **Materials and Methods**

420 **Seedlings and experimental design**

421 Our study focused on two tree species commonly found in the Mediterranean region
422 and naturally co-occurring over large areas: the isohydric Aleppo pine (*P. halepensis*,
423 drought avoidant with tight water loss control) and the anisohydric holm oak (*Q. ilex*,
424 drought tolerant with more progressive water loss control). The experiment compared
425 water status and hydraulic traits during drought among seedlings grown in mixture
426 and monocultures, and with or without physical barrier preventing intimate root
427 contact among the two plants (see below). This latter treatment aimed at testing
428 whether the root systems of the two species need to be entangled to observe mixture
429 effects, or if soil matrix potential gradients are large enough to trigger mixture effect
430 without a close contact between root systems.

431 From 2019 to June 2021, saplings were grown at the French National Forestry Office
432 of France (ONF) nursery in Cadarache (Southeast of France) and were watered twice
433 a week to field capacity and fertilized once a week. Seedlings of *P. halepensis* and *Q.*
434 *ilex* (one- and two-years old respectively) of equivalent dimensions were repotted in
435 January 2020. 90 trees of each species were planted in 12 L containers, each
436 containing two individuals per pot, either in monoculture or in mixtures. The soil was
437 composed mainly of organic matter and of sand (~20%). Half of the pots were
438 equipped with a physical barrier made of acrylic fabric with a 30µm mesh that
439 precluded root colonization from one side to the other of the pot but allowed water
440 transfer between the two separated compartments. One month before the start of the
441 experiment (June 2021), pots were brought on the campus of INRAE in Avignon
442 (Southeast France) to acclimate in the experimental greenhouse. The greenhouse was
443 equipped with air temperature, humidity (HD 9817T1) and radiation loggers. It
444 included an independent regulation of climate through aeration (window opening or

445 forced ventilation) and cooling (humidification of the air entering through a “cool
 446 box”). These systems allowed regulating the environment of the greenhouse
 447 according to the defined settings. In addition, the sidewalls of the greenhouse had
 448 been whitewashed to homogenize the radiation and the temperature. The temperature
 449 was kept between 25 and 35 °C, relative humidity (RH) between 40 and 75%, and
 450 maximum diurnal photosynthetically active radiation (PPFD) below 1000 $\mu\text{mol.m}^{-2}.\text{s}^{-1}$
 451 (Figure S1).

452 During the acclimation period in the greenhouse, watering was applied as in the
 453 nursery. Among the initial batch of 90 pots, we selected 54 pots for which the two
 454 trees were alive and had reached a height between 40 and 60 cm with less than 10 cm
 455 height differences between the two trees. Pots were divided into two batches: a batch
 456 of 6 pots per composition (36 pots in total) that was assigned to the drought
 457 experiment, and a batch of 3 pots per treatment (18 pots in total) that was assigned to
 458 a control treatment in which trees were maintained watered all along the season (two
 459 times a week). The day before the beginning of the experiment, at the end of the
 460 afternoon, all pots were watered at saturation and weighted.

461 The experiment was set up during the summer 2021. It consisted in applying a
 462 drought treatment (watering stop) to potted *P. halepensis* and *Q. ilex* trees grown in
 463 monoculture or in mixture while monitoring ecophysiological variables at 5 different
 464 dates. All pots were monitored once a week, from July 26 to August 18, for leaf water
 465 potentials, leaf gas exchanges, and pot weights.

466 **Plant water potentials measurements**

467 Water potentials were measured at predawn once a week across the experimental
 468 period for all trees monitored. The evening before measurements one leaf (*Q. ilex*) or
 469 small twig (*P. halepensis*) of each tree was covered with an aluminium foil and placed
 470 in a ziplock plastic bag. In addition, to limit tree nocturnal transpiration and allow
 471 water potential equilibration between the tree and the soil (Rodriguez-Dominguez et
 472 al., 2022), trees were covered with a plastic bag and a piece of wet paper was included
 473 under the plastic bag. Samples were collected before sunrise, between 4 to 5 am, kept
 474 into the ziplock and immediately placed in a cooler for water potential measurement.
 475 The 108 measurements were done randomly in less than 4 hours following sampling,
 476 with a Scholander pressure chamber (PMS model 1505 D).

477 **Tree leaf gas exchanges**

478 Leaf level gas exchanges were measured using two portable photosynthesis system
 479 (LI-6400XT) for all trees at all dates except the second one due to a breakdown of the
 480 greenhouse system affecting cooling system. Measurements were done between 11
 481 am to 3 pm, period during which PAR in the green house was highest and stable
 482 (between 600 and 1000 $\mu\text{mol.m}^{-2}.\text{s}^{-1}$). Licor chamber conditions were set to keep
 483 close to the greenhouse while providing non-limiting conditions: PAR was set at 1000
 484 $\mu\text{mol.m}^{-2}.\text{s}^{-1}$, the block temperature was set at 25°C, flow rate and scrubbing were
 485 adjusted to maintain RH between 60 and 80%. The leaves were allowed to acclimate
 486 for at least 3 minutes in the chamber before measurement, to ensure gas exchange
 487 stability. For each leaf (*Q. ilex*) or needle bunch (*P. halepensis*), ten values were
 488 recorded during one minute and the average was used in the data analysis. After the
 489 measurement, the area of leaves or needles included in the chamber were cut and
 490 stored in a plastic bag inside a cooler. The day after, leaf area was measured to correct

491 gas exchange computation with actual leaf area in the chamber. Samples were then
 492 dried during 48 hours at 70°C to estimate specific leaf area.

493 **Tree biomass and leaf area estimates**

494 We estimated leaf area of each tree at the beginning and the end of the experiment
 495 using a method relying on profile photographs, adapted from (Ter-Mikaelian and
 496 Parker, 2000). It is based on a calibrated relationship between the projected area of the
 497 tree profile and the foliage biomass estimated destructively. For each species, we first
 498 built a calibration relationship between the number of tree pixels in profile
 499 photographs and the foliage biomass. For the calibration relationship, trees were
 500 selected to span the range of sizes encountered in the experiment. We sampled trees
 501 before the beginning of the drought experiment (June 2021), but also after the
 502 experiment (September 2021), to account for potential changes in size or leaf area or
 503 angulation that could have occurred during the summer and influenced the
 504 relationship. For each tree, the profile surface projected area was estimated by
 505 photography. All the settings were made to ensure a constant reproduction ratio (i.e.,
 506 constant dimensions of real object dimensions per pixel) among photographs. To
 507 obtain foliage dry mass, all trees used for this calibration were cut at the base of the
 508 stem after taking the photographs. Tree parts were sorted to separate green foliage,
 509 dead foliage, and the rest which was almost entirely made of stems. Tree parts were
 510 then dried at 70°C for 3 days (leaves/ needles) or until there was no variation in dry
 511 mass (almost one week). The leaf area of each tree was computed by converting
 512 foliage dry mass into area using specific leaf areas estimated on leaf gas exchange
 513 measurement samples.

514 At the end of the experiment and for droughted pots, the belowground part of each
 515 tree was uprooted. The rooting system was washed to separate the soil particles from
 516 the roots. Each plant was hung vertically, and the rooting system extension (maximal
 517 length and width) was measured using a ruler, with a millimeter resolution. The root
 518 system was then dried out at 70°C in an oven for at least 10 days, until there are no
 519 more weight variations, and the total dry mass was estimated.

520 **Soil water content and soil water potentials**

521 Pots were weighted at each measurement dates in the morning (ca. 8 AM) and at the
 522 end of the measurement day (ca. 5 PM). Soil water content was estimated at the pot
 523 level, by subtracting the total pot weight (measured in the morning) by the soil dry
 524 mass and the total fresh tree biomass. Soil water potential (Ψ_{soil}) was then estimated at
 525 the pot level from the normalized soil water content of the pots (W_{norm}) and water
 526 retention curves determined in the laboratory on soil samples ($V = 6 \text{ cm}^3$). The
 527 determination of the retention curve was made with the combination of suction table
 528 ($\Psi_{\text{soil}} > -0.01 \text{ MPa}$), pressure plate ($\Psi_{\text{soil}} > -1.5 \text{ MPa}$) and dew point hygrometer
 529 (WP4C, Decagon- $\Psi_{\text{soil}} < -1.5 \text{ MPa}$) methods (Dane and Topp, 2020). Five soil
 530 sample replicates were used for each point of the retention curve and the gravimetric
 531 water content was determined from fresh and dry weight obtained after drying in an
 532 oven at 70°C (temperature limit to avoid organic matter degradation) for about one
 533 week. To perfectly match the data, two different retention curves using van-
 534 Genuchten relationships (van Genuchten, 1980) were fitted. A first retention curve
 535 was fitted with gravimetric water contents above $0.1214 \text{ g} \cdot \text{g}^{-1}$ (corresponding to Ψ_{soil}

536 = -1.25 MPa). For gravimetric water content lower than 0.1214 g. g⁻¹, a second of
537 retention curve was fitted. The retention curves take the following form:

$$538 \quad \psi_{soil} = \frac{\left(\left(\frac{1}{\theta}\right)^{\frac{1}{m}-1}\right)^{\frac{1}{n}}}{\alpha} \quad (1)$$

539 Where m , n and α are empirical parameters describing the typical sigmoidal shape of
540 the function and θ is the normalized water content. Water potentials were calculated
541 from this fit using the gravimetric water contents of pots estimated at each
542 measurement dates. The parameters of the curves are provided in Figure S8 and Table
543 S4.

544 The normalized water content (θ) was computed for each pot as:

$$545 \quad \theta = \frac{W - W_r}{W_{sat} - W_r} \quad (2)$$

546 With W the gravimetric water content of the pot at a given time, W_r the residual
547 gravimetric water content and W_{sat} the gravimetric water content at saturation. It
548 was measured at the end of the experiment after drying the soil at 70°C. W_{sat} was
549 estimated from the first weight measurement of the experiment, after the pots were
550 irrigated at saturation. W and W_{sat} were computed by removing the mass of the tree
551 and the pot to the total weight measured during the experiment. The total tree weight
552 was measured at the end of the experiment, by assuming that tree growth that could
553 have occurred during the experiment can be neglected due to the extreme drought
554 experienced by the tree.

555 Since soil water potentials were not directly measured, we calculated soil water
556 potentials from water contents as described above, and also plus or minus the largest
557 error possible combining both the retention curve precision and the weighting
558 uncertainty (Figure S4). The largest difference between measurements and the fitted
559 van Genuchten curves in the [-6, 0] MPa range (a range consistent with our
560 experiment) was 0.63 MPa. The scale used to weight the pots had a measurement
561 precision of ± 0.5 g. We then compared tree water potentials to the three estimates of
562 soil water potentials (Figure S4).

563 **Soil resistivity measurement**

564 Electrical resistivity of soil in pots was measured using electrical resistivity
565 tomography (ERT). 4 pots (including one control) per modality (monoculture or
566 mixture, with or without root separation system) were selected. On these pots,
567 electrical resistivity was monitored with time over 2 radial planes, located at 1/3 and
568 2/3 of the pots' height, by inserting 20 stainless steel screws (2cm long) equally
569 spaced (3.9cm) along the column's circumference. ERT measurements were done
570 using an ABEM SAS 4000 resistivity meter connected to all these electrodes. All
571 quadrupole combinations were used, including reciprocal measurements for assessing
572 error and measurement quality. The resistivity measurements were taken before the
573 start of the experiment (when the pot substrates were at field capacity), in the middle
574 and at the end of the experiment. In the late dry situations, it was necessary to add a
575 small amount of water at electrodes to enable soil-electrode electrical contact and
576 resistivity measurements. Soil resistivity distribution at the two heights was obtained

577 from the inversion of apparent resistivity using ResIPy software (Blanchy et al.,
578 2020).

579 **Statistics**

580 We evaluated the effect of species and measurement date and their interactions on the
581 water potential of trees by using a linear mixed model. Then, for each species
582 independently and root separation modalities (root separation or not), we assessed the
583 effect of pot composition (mixture or monoculture association) on predawn water
584 potentials by considering date, composition and their interaction as explanatory
585 factors. As we did not find any significant differences between water potentials of
586 monoculture with and without root separation for each species (Figure S9), we
587 decided to pool them for the analysis. We also tested the differences between soil and
588 tree water potentials at each measurement date using Student T tests. Finally, we
589 applied post-hoc Tuckey HSD tests to evaluate differences between pots modalities
590 (composition and root separation) for gas exchange variables (leaf conductance and
591 transpiration, Figure S3). All statistical analyses were performed with the R software
592 (3.5.2, R Development Core Team 2018) with the packages lme4 and agricolae (Bates
593 et al., 2023; Mendiburu, 2023).

594 **Model analysis using SurEau**

595 *General overview of the model*

596 We performed sensitivity analysis with a soil-plant hydraulic model in order to
597 explore the mechanisms driving the mixture effects during an extreme drought. We
598 used the SurEau model coded in C, which has been extensively presented previously
599 (Cochard et al., 2021). In brief, SurEau has been designed to model extreme drought
600 and accounts for the processes occurring after the point of stomatal closure (*i.e.*,
601 cuticular water losses as well as losses of hydraulic conductance and plant water
602 stocks due to xylem embolism). It computes water fluxes along a discretized soil-tree
603 atmosphere continuum and accounts for variations of plant and soil water stocks and
604 water potential (which are the state variables of the model) by using diffusion laws
605 (conductance and water potential gradients between compartments) and capacitances.
606 The model is driven by hourly climate data (temperature, VPD, radiation, wind
607 speed), which are downscaled at smaller time step to perform computation. At each
608 time step, the model starts with the computation of leaf stomatal and cuticular
609 transpiration as the product between leaf-to-air vapor pressure deficit and stomatal
610 and cuticular conductance. These fluxes are used to trigger a drop in water content in
611 the leaves, which is translated into a water potential drop (using the specific
612 capacitances). In turn, leaf water potential is used to compute water flows with the
613 adjacent compartments and update their water potential and water quantities. This
614 approach is applied to all compartments (including the soil) over one small-time step
615 to avoid numerical instabilities (ca. 0.01s; (Ruffault et al., 2022) and repeated until the
616 plants eventually reach total hydraulic failure (loss of xylem conductance) in all
617 apoplasmic compartments.

618 Stomatal conductance (g_s) was modelled using a Jarvis formulation, by which g_s
619 depends on radiation and leaf water potential (Cochard et al., 2021). The leaf stomatal
620 response to water potential was set species specific as in (Martin-StPaul et al., 2017).
621 The leaf cuticular transpiration is modelled as a result of the product between vapor

622 pressure deficit and leaf cuticular conductance (g_{cuti} , which by default was set
623 constant for each species).

624 The soil is discretized into three soil layers and the plant system into four organs
625 (roots, trunk, branches, and leaves). Each plant organ is composed of an apoplastic
626 (i.e., xylem) and a symplasmic compartments, each being defined by a capacitance
627 and conductance with the surrounding compartments. The capacitance of the
628 symplasm depends on the water potential according to the pressure volume curves;
629 whereas the capacitance of the apoplasm is set constant (Cochard et al., 2021; Martin-
630 StPaul et al., 2017). The organs are connected between each other axially via their
631 apoplasm and each organ's apoplasm is connected radially with a symplasm. The
632 hydraulic conductance of the xylem (apoplasm can decline as a result of xylem
633 embolism. Xylem embolism is computed by using the xylem vulnerability curve to
634 cavitation. Each soil layer is connected to a root in series, and all roots are connected
635 to the trunk in parallel. The soil hydraulic conductivity and the soil water potential of
636 each layer are computed as a function of soil water quantity and the saturated
637 conductivity using the van Genuchten model (van Genuchten, 1980). The hydraulic
638 conductance between the soil and the fine roots for each soil layer is computed by
639 using the soil conductivity and the scaling factor (B_{GC}) based on fine root density
640 proposed by Gardner-Mualem, as described in (Martin-StPaul et al., 2017):

$$641 \quad k_{soil} = B_{GC} \cdot K_{sat} \cdot REW \times \left[1 - \left(1 - REW^{\frac{1}{m}} \right)^m \right]^2 \quad (3)$$

642 with K_{sat} the soil hydraulic conductivity at saturation, m a parameter from the van
643 Genuchten soil water retention curve, REW the relative water content ($REW = \frac{\theta - \theta_r}{\theta_s - \theta_r}$,
644 with θ the actual soil water content, θ_r the residual soil water content and θ_s the soil
645 water content at saturation), and B_{GC} the scaling factor calculated as:

$$646 \quad B_{GC} = \frac{2\pi \cdot La}{\ln\left(\frac{1}{r\sqrt{\pi} \cdot Lv}\right)} \quad (4)$$

647 with La and Lv the root length per soil area and volume, r the radius of fine roots. The
648 root length was the target of sensitivity analysis (see below sensitivity analysis).

649 Each fine root is connected to the soil layer through a symplasmic conductance which
650 is set constant by default (K_{root}). This root symplasmic conductance has been modified
651 in the sensitivity analysis to test the effect of plant isolation from the soil during
652 drought (see below sensitivity analysis).

653 In the present study, the model was improved to include the possibility for two trees
654 to absorb water in the same soil volume. In principle, two codes corresponding to two
655 trees, parameterized for monoculture of *P. halepensis*, monoculture of *Q. ilex* or for
656 mixture, were run in parallel.

657 *General considerations about the model parametrization and application*

658 We describe below the main parameters used in this study and refer the reader to
659 Cochard et al (2021) for further information about parameters definitions and their
660 implementations. The parameters can be separated into three types:

661 (1) plant size-related traits including (i) the hydraulic conductance for the
662 different plant compartments, (ii) the water volumes of the different

663 compartments, (iii) the overall leaf area and fine root length and area. These
 664 parameters can be derived from direct measurements and from allometric
 665 relationships.

666 (2) physiological traits including (i) the pressure volume curves parameters (π_{100} ,
 667 ϵ), (ii) the vulnerability curve to cavitation (P50, slope), (iii) the stomatal
 668 response to radiation and to water potential, (iv) the leaf cuticular
 669 conductance.

670 (3) soil parameters including the soil depth and the water retention curves
 671 parameters (van Genuchten equation parameters) for each soil layer.

672 In the simulations made for this study, size related parameters were set constant for
 673 the two species. We assumed each plant to be small plant of 1m of height with a stem
 674 diameter of 1cm and a leaf area 0.2 m². The volumes of water of the different woody
 675 compartment (branches, trunk, and leaves) were computed assuming a branch to trunk
 676 ratio of 0.5 and a root to shoot ratio of 0.3. The volume of water in the leaves were
 677 computed based on the leaf area and a succulence of 100 g/m². The default fine root
 678 area was set equal to the leaf area (assuming a fine root to leaf area ratio of 1). The
 679 fine root length was computed assuming a fine root diameter of 0.5mm and
 680 distributed equally among the three soil layers.

681 The hydraulic conductance of the different compartments was defined by using a total
 682 leaf specific hydraulic conductance around 1 mmol/m²/s/MPa (value for small trees
 683 consistent with our measurements and with the previous literature, (Mencuccini,
 684 2003) which was distributed among the plant compartments assuming a typical
 685 hydraulic architecture (Cruziat et al., 2002; Tyree and Ewers, 1991). The hydraulic
 686 resistance was thus distributed as follows: 20% in the leaf symplasm, 20% in the leaf
 687 apoplasm, 8% in the branch apoplasm, 2% in the stem apoplasm, 10 % in the root
 688 apoplasm and 40% in the root symplasm. The radial symplasmic resistance was
 689 computed for each woody compartment (roots, trunk, branch) using the developed
 690 areas and a symplasmic conductivity of 1 (mmol.m⁻². s⁻¹. MPa⁻¹) for trunk and
 691 branches and 3.5 (mmol.m⁻². s⁻¹. MPa⁻¹) for roots (Cochard et al., 2021). Note that the
 692 root symplasmic hydraulic conductance (K_{root}) dictates the water fluxes between the
 693 soil and the inner part of the root was the target of sensitivity analysis (see below).

694 The physiological traits used in the model to define the water use and drought
 695 resistance strategies of the two studied species were set by using previously published
 696 literature or personal data (Table 4). For the sake of simplicity, potential segmentation
 697 of xylem vulnerability was omitted and the same vulnerability curve to cavitation was
 698 used for all compartments of the same species. Similarly, the same species-specific
 699 leaf PV curve was used to compute the symplasmic capacitance of all the symplasmic
 700 compartments. The stomata response to leaf symplasmic water potential used in the
 701 model for water loss regulation was set by using published data of concurrent
 702 measurements of stomatal conductance and leaf water potential (Klein, 2014; Martin-
 703 StPaul et al., 2017). The maximum stomatal conductance and the stomata response to
 704 incident PAR were set constant among species as in (Ruffault et al., 2022). The leaf
 705 cuticular conductance was taken from (Billon et al., 2020). It is based on
 706 measurement of leaf water loss under controlled climatic conditions, averaged after
 707 the point of stomatal closure. This value has also been the target of a sensitivity
 708 analysis (see below).

709 Since not all the parameters of the specific soil used in the experiment have been
 710 measured, the soil hydraulic parameters (Table 5) were taken from a typical French

711 Mediterranean site where the SurEau model was previously applied (Ruffault et al.,
 712 2023). However, to generalize our results, a sensitivity analysis was made for a large
 713 range of soils using parameters from (Carsel and Parrish, 1988; Figure S10; Table
 714 S5). For each simulation (in monoculture and mixture with the different soil
 715 parameters) we used the time to hydraulic failure (THF) computed by the model as an
 716 indicator of drought stress resistance. THF corresponds to the modelling time required
 717 for the plant to reach water potential causing 100 % loss of hydraulic conductivity.
 718 For each type of soil and each species, we computed the relative time to hydraulic
 719 failure in mixture compared to monoculture as $THF_{relative} = THF_{mixtures} /$
 720 $THF_{monoculture}$. A value of 1 means that mixture and monoculture experienced the
 721 same water stress. The results (Figure S10) highlight an overall consistent pattern
 722 (regardless of the soil type) with our current results: in mixture, hydraulic risk (i.e.,
 723 THF) increase for *Q. ilex* and decreased for *P. halepensis*.

724 The model was initialized with a soil at the field capacity. Then, the model was forced
 725 with constant climatic conditions from day to day, but variable diurnally as in
 726 (Cochard et al., 2021; Ruffault et al., 2022). The rainfall was set to 0 to explore a
 727 desiccation dynamic as in the experiment. Simulations were stopped when the two
 728 plants reached total hydraulic failure (defined as 100% loss of conductivity in the
 729 stem). The time to reach hydraulic failure (THF) was used as an index of drought
 730 stress resistance to compare the species and treatments (mixture and monocultures).

731

732 *Hypothesis testing using SurEau model sensitivity analysis*

733 1- Benchmark simulations

734 To test the hypotheses presented in the introduction (illustrated in Figure 1B) we first
 735 performed *benchmark* simulations. Simulations with two individuals in monoculture
 736 or mixture competing for the same amount of water, were performed using the default
 737 parameters described in the section above (Table 4). The results obtained with these
 738 simulations were in accordance with the hypothesis drawn in Figure 1B but departed
 739 from the empirical results. Indeed, these simulations were unable to reproduce the
 740 relatively constant water potential of the isohydric *P. halepensis* species during
 741 extreme drought. As explained above, the patterns of Figure 1B hold only under the
 742 assumptions that (i) there is no significant segregation in soil exploration by the two
 743 species (which is reasonably the case of our experiment as we observed that root
 744 systems of the two species colonized the full soil volume, which was set low on
 745 purpose), (ii) that the two individuals are highly connected to the soil (i.e. large
 746 hydraulic conductance between the soil and the fine roots).

747 Consequently, we performed different types of sensitivity analysis with SurEau in
 748 order to explore how changes in soil or root hydraulic conductance could help to
 749 represent the observed empirical patterns. The water flow between the soil and inner
 750 part of the root being modelled using two different conductance (K_{soil} and K_{root} , see
 751 above), these two conductances were modulated as described below.

752 2- Testing the “isolation effect” for *P. halepensis*: Can we explain the relatively
 753 constant water potential of *P. halepensis* with variable root hydraulic
 754 conductance (K_{root}) and cuticular conductance (g_{cuti})?

755 For *P. halepensis* empirical data support that plant water potential can be higher than
 756 soil water potential during extreme drought, suggesting that this species can behave
 757 independently from the soil and maintain its water potential constant even if soil

758 water potential decreases. Previous studies suggested that decline in conductance
 759 between the soil and root can occur during drought (Cuneo et al., 2016; Duddek et al.,
 760 2022; North and Nobel, 1997). This can be represented in the model by decreasing the
 761 root symplasmic conductivity when root water potential decreases. Therefore, we
 762 implemented a variable K_{root} by assuming a variable gap fraction in the root cortex:

$$763 \quad K_{root} = \frac{K_{root_{symp0}} * (100 - Cortex_{Gap})}{100}$$

764 (5)

765 With $K_{root_{symp0}}$ the initial hydraulic symplasmic conductivity and $Cortex_{Gap}$ the
 766 proportion of gap in the root cortex, which we computed by assuming a sigmoidal
 767 dependence to the root symplasmic water potential $P_{root_{symp}}$:

$$768 \quad Cortex_{Gap} = \frac{100}{(1 + \exp(K_{varP2} / 25 * (P_{root_{symp}} - K_{varP1})))}$$

769 (6)

770 with K_{varP1} the water potential causing 50% of cortex gap and K_{varP2} the slope at the
 771 point of inflexion of the sigmoid (Figure S5).

772 We used this implementation to perform simulation in mixture conditions, still
 773 parametrizing $Q. ilex$ as in benchmark conditions. Such implementation led to an
 774 acceleration of hydraulic failure for *P. halepensis*, which is explained by the fact that
 775 there is less water supply from the soil, but still significant cuticular losses that are not
 776 anymore be compensated, and thus lead to an excessive plant desiccation. We
 777 therefore also tested whether accounting for a concurrent decrease in leaf cuticular
 778 conductance during drought stress, a phenomenon already observed on cut branches
 779 of *P. halepensis*, could explain -- alone or in combination with the reduction in root
 780 conductance -- the observed pattern (Figure S6 A). To do so, we implemented a linear
 781 decrease of the cuticular conductance (g_{cuti}) with the leaf symplasmic relative water
 782 content (RWC, Figure S6 B) as observed for *P. halepensis* using a drought-box
 783 (Billon et al., 2020). We assumed that after turgor loss point, g_{cuti} decreased linearly:

$$784 \quad \text{if}(RWC_{leaf} < RWC_{tlp})$$

$$785 \quad g_{cuti} = g_{cuti_{ref}} * (1 - (RWC_{tlp} - RWC_{leaf}) * RWC_{sens})$$

786 (7)

$$787 \quad \text{else } g_{cuti} = g_{cuti_{ref}}$$

788 With RWC_{leaf} the leaf symplasmic relative water content, RWC_{tlp} the leaf relative
 789 water content at turgor loss point, RWC_{sens} the sensitivity of g_{cuti} to relative water
 790 content, $g_{cuti_{ref}}$ the reference leaf cuticular conductance. We found that combining
 791 both, a reduction of K_{root} and a reduction of $g_{cuti_{ref}}$ led to patterns of water potential
 792 consistent with our empirical findings.

793 3- Testing the potential increase of soil hydraulic conductance through increased
 794 root length for *Q. ilex* in mixture

795 Secondly, for *Q. ilex*, we noticed a lower water stress under mixture which was also
 796 linked to a change in the relationship of the soil water potential (Ψ_{soil}) vs plant

797 predawn water potential (Ψ_{pd}). Higher plant water potential for a given soil water
 798 potential was found under mixture compared to monoculture. Such pattern could be
 799 explained by an increase of the soil hydraulic conductance that, as evidenced by
 800 equations 3 and 4, can be related to the density of fine roots (L_a and L_v , the length of
 801 fine roots per m^2/m^3 of soil). It is also consistent with the observed increase in root
 802 length under mixture conditions (Figure S7). We therefore performed a sensitivity
 803 analysis to the density of fine roots under monoculture conditions to test whether this
 804 trait changes explains the observed mixture effect on water status.

805

806 **Supplementary Data**

807 **Supplementary Figure S1.** Meteorological variables recorded in the greenhouse
 808 during the experimentation: relative humidity, photosynthetic active radiation (PAR),
 809 and temperature.

810 **Supplementary Figure S2.** Mean resistivity of the top and bottom profiles of pots
 811 (1/3 and 2/3 of the height of a given pot) at the end of the experiment according to pot
 812 modality.

813 **Supplementary Figure S3.** Dynamics of leaf transpiration and conductance for *Q.*
 814 *ilex* (QI) and *P. halepensis* (PH), either in monocultures (black dots) or mixtures (grey
 815 dots), without (left panel) or with (right panel) root separation.

816 **Supplementary Figure S4.** Impact of soil water potential computation uncertainty on
 817 the difference between soil and tree water potentials.

818 **Supplementary Figure S5.** Relationship between root hydraulic conductance (K_{root})
 819 and root symplasmic water potential implemented in the sureau model simulations to
 820 test the hypothesis of soil to root isolation for *P. halepensis*.

821 **Supplementary Figure S6.** Relationship between the leaf cuticular conductance
 822 (g_{cuti}) and the leaf relative water content used to test the hypothesis of leaf to air
 823 isolation for *P. halepensis*.

824 **Supplementary Figure S7.** Average root length of *Q. ilex* (grey bars) and *P.*
 825 *halepensis* (white bars) for the different pot composition modalities.

826 **Supplementary Figure S8.** Soil water retentions curves obtained on subsamples of
 827 soil and used to extrapolate soil water potential (or soil matric potential, h) of the pots.

828 **Supplementary Figure S9.** Averages and standard deviations of plant predawn water
 829 potentials (Ψ_{pd}) in monocultures.

830 **Supplementary Figure S10.** Time to hydraulic failure (THF) of both species relative
 831 to monoculture (relative THF = $THF_{mixture} / THF_{monoculture}$, a value of 1 - shown
 832 by the dashed red line - indicates that mixture and monoculture experience the same
 833 water stress) in the soil type given by Carsel & Parrish 1988, and for the Puéchabon
 834 soil used for simulation.

835 **Supplementary Table S1.** Analysis of variance of the mixed model for tree predawn
 836 water potential to test date and species effect.

837 **Supplementary Table S2.** Analysis of variance of the mixed models to test the
 838 composition effect (monoculture vs mixture), per species and type of pot (with or
 839 without root separation), for tree water potential (measured at predawn).

840 **Supplementary Table S3.** Water flux estimate between the compartment of the pots
 841 at the penultimate and last dates of measurement.

842 **Supplementary Table S4.** Parameters of the retention curve for the first ($\Psi_{\text{soil}} <$
 843 12.5 bar) and second ($\Psi_{\text{soil}} > 12.5$ bar) fits of the van Genuchten equation.

844 **Supplementary Table S5.** Soil parameters describing the water retention curves
 845 according to soil types given by Carsel & Parrish 1988.

846 **Supplementary Method S1.** Computation of water fluxes between the two pots
 847 compartments of the mixture with root separation modality.

848

849 **Funding**

850 Myriam Moreno was supported by the French Environment and Energy Management
 851 Agency (ADEME) in the form of a PhD scholarship. The experiment was funded by
 852 Agence Nationale pour la Recherche (MixForChange, ANR-20-EBI5-0003; TAW-
 853 tree, ANR-23-CE01-0008-01) and the Metaprogramme ACCAF Drought&Fire.

854

855 **Acknowledgments**

856 We would like to thank the ONF-PNRGF (Pôle National des Ressources Génétiques
 857 Forestières de l'Office National des Forêts) nursery of Cadarache (13) for caring for
 858 the plants two years prior to the experiment. Thanks also to Gilles Vercambre and the
 859 greenhouse staff of the PSH unit, for accompanying us during the experiment. Finally,
 860 thanks to the URFM and EMMAH inrae staff, in particular to Henri Picot, Denis
 861 Portier, Arnaud Jouineau, Marion Parizat, Didier Besombes, Didier Betored, Philippe
 862 Petit, Arnaud Chapelet, and to Anouk Brisset and Léo Corridor (students), for their
 863 help in the setting up of the experiment and acquiring data.

864

865 **Author Contributions**

866 M.M., N.K.M-S and H.C designed the research; F.J. and O.M. helped in the setting up
 867 of the experiment. In particular, F.J. coordinated the cooperation with the ONF-
 868 PNRGF (Pôle National des Ressources Génétiques Forestières de l'Office National
 869 des Forêts) nursery of Cadarache (13) and secured a site in the greenhouse. O.M.
 870 controlled and installed devices used for the measurements; M.M. and N.K.M-S
 871 performed research with the help of C.D, R.D., G.S. and P.F-C; H.C. and N.K.M-S
 872 performed the model simulations; M.M. analyzed the data with the help of N.K.M-S,
 873 G.S., C.D and H.C.; M.M. write the first draft of the manuscript, which was then
 874 modified by both N.K.M-S and M.M. All authors contributed to review the
 875 manuscript and approved the final version.

876

877 **Table 1:** F statistics and *p* values of factors in the analysis of variance model of the
 878 predawn water potentials of both species according to pot modalities (monoculture or
 879 mixture, with or without root separation) and soil water potentials (Ψ_{soil}). Summary
 880 of linear mixed effect model of the predawn water potentials of both species
 881 according to pot modalities (monoculture mixture with or without root separation) and
 882 soil water potentials (Ψ_{soil}) using monoculture as reference.

Factors	<i>Q. ilex</i>		<i>P. halepensis</i>	
	F_value	P_value	F_value	P_value
Ψ_{soil}	824.83	< 2.2e-16	707.69	< 2.2e-16
Pot modalities	30.24	11.38 e-11	1.84	0.1
Ψ_{soil} : Pot modalities	17.26	2.12e-07	1.89	0.15

883

884

885

886 **Table 2:** Summary of linear mixed effect model of the predawn water potentials of
 887 both species according to pot modalities (monoculture mixture with or without root
 888 separation) and soil water potentials (Ψ_{soil}) using monoculture as reference.

Factors	<i>Q. ilex</i>		<i>P. halepensis</i>	
	T_value	P_value	T_value	P_value
Intercept	-1.489	0.139	-7.904	1.3e-12
Ψ_{soil}	25.77	< 2e-16	21.318	< 2e-16
Mixture with root sep	0.03	0.98	0.06	0.95
Mixture without root sep	0.63	0.53	0.21	0.83
Ψ_{soil} : Mixture with root sep	0.32	0.75	1.77	0.08
Ψ_{soil} : Mixture without root sep	-5.64	9.71e-08	-0.45	0.65

889

890 **Table 3:** F statistics and *p* values of factors in the analysis of variance of the predawn
 891 water potentials of *Q. ilex* (Ψ_{pd} QI) in mixtures according to predawn water potentials
 892 of *P. halepensis* (Ψ_{pd} PH) and root separation modality (with or without root
 893 separation) (Ψ_{pd} QI~ PH*Separation modality)

894

Factors	F_value	P_value
Ψ_{pd} PH	338.1	< 2.2e-16
Separation modality	10.9	0.002
Ψ_{pd} PH: Separation modality	5.14	0.03

895

896

897

898

899 **Table 4:** Species specific parameters used in the model to describe the water use and
 900 drought tolerance strategies of the species.

901

Traits (symbol. units)	<i>P. halepensis</i>	<i>Q. ilex</i>	Comments	References
Water potential causing 10% stomatal closure (Ψ_{gs_10} . MPa)	-1.5	-1	/	Martin-StPaul et al 2017
Water potential causing 90% stomatal closure (Ψ_{gs_90} . MPa)	-2.5	-4	/	Martin-StPaul et al 2017
P50 of the xylem of the vulnerability curve (MPa)	-4.7	-7.1	Constant for all apoplasmic organs	(Sergent et al., 2020); Martin-StPaul et al 2017
Slope of the xylem vulnerability curve (%/MPa)	78	23	Constant for all apoplasmic organs	Sergent et al 2020; Martin-StPaul et al 2017
Osmotic potential at full turgor (π_{100} . MPa)	-1.26	-1.9	Constant for all symplasmic organs	Martin-StPaul et al 2017; Moreno, 2022
Modulus of elasticity of the symplasm (ϵ . MPa)	9.7	16	Constant for all symplasmic organs	Martin-StPaul et al 2017; M. Moreno, 2022
g_{cuti_ref} ($mmol.m^{-2}.s^{-1}$)	1.1	2.38	Targeted for a sensitivity analysis	Billon et al 2020; M. Moreno, 2022
Leaf area (m^2)	0.17	0.14	Constant	This study
Succulence ($gH_2O.m^{-2}$)	300	145	/	Ruffault and Martin-StPaul, 2024
K_{plant} (Leaf specific. $mmol.m^{-2}.s^{-1}.MPa^{-1}$)	0.8	1.4	/	This study

902 **Table 5:** Soil parameters (Puéchabon site) describing the water retention curves and
 903 the changes in soil conductivity, used for all three soil layers in Sureau simulations.

θ_{sat}	θ_r	α	n	K_{sat} (mol/s/MPa)
0.28	0.1	0.0005	2	5

904

905

906 **Figure 1.** Conceptual representation of drought effects on hydraulic risk of
 907 monocultures and mixtures, for two species with contrasting water use strategies.

908 (A) Drought responses of species according the resistance strategy they adopt. During
 909 drought, the *isohydric* species (i.e., *Pinus halepensis*, also referred as drought
 910 avoidant) close its stomata at a relatively high-water potential (Ψ_{close} , corresponding to
 911 the water potential inducing full stomatal closure) and has a low cuticular
 912 conductance (g_{cuti}). Also, it has a relatively high P50 (water potential causing 50 %

913 loss of hydraulic conductivity), making it more vulnerable to xylem cavitation.
914 Whereas, the *anisohydric* species (i.e., *Quercus ilex*, also referred as drought tolerant),
915 has a lower Ψ_{close} and a higher g_{cuti} , making it consuming more water. Additionally, it
916 has a lower P50 (water potential causing 50 % loss of hydraulic conductivity), making
917 it more resistant to xylem cavitation.

918 (B) Experimental design and hypothesized drought responses for monocultures and
919 mixtures of an *isohydric* (drought avoidant) and an *anisohydric* (drought tolerant)
920 species. The transpiration, water potentials (Ψ_{soil} : overall pot soil water potential; Ψ_{pd} :
921 plant predawn water potential) and hydraulic safety margins (HSM) for each situation
922 and species. HSM represents the risk of hydraulic failure, it generally refers the
923 difference between the minimum plant water potential and vulnerability to cavitation
924 (P50, the water potential causing 50 % of embolism). In the *isohydric* monoculture,
925 tree transpiration is expected to reduce rapidly after the onset of drought, limiting the
926 drop in Ψ_{soil} and Ψ_{pd} , and hence the hydraulic failure risk (positive HSM). In the
927 *anisohydric* monoculture, transpiration should decrease later as stomatal control is
928 expected to be more released than the one of the *isohydric* species. This should trigger
929 a steeper decrease of Ψ_{soil} and Ψ_{pd} , thereby increasing the risk of hydraulic failure
930 (more negative HSM). In the mixture without root separation, transpiration of the
931 *isohydric* should decrease earlier than for the *anisohydric*. This is expected to dampen
932 overall soil water loss and thus Ψ_{pd} and HSM of the *anisohydric* species compared to
933 the monoculture. However, the water consumption of the *anisohydric* continue
934 beyond the point of stomatal closure and of cavitation of the *isohydric*. This triggers a
935 decrease of steeper decline of Ψ_{pd} and HSM for the *isohydric* compare to
936 monoculture. A mixture with root separation illustrates that when each species root
937 system occupies its proper soil volume, the regulation of the transpiration, the water
938 potentials dynamics and the HSM are expected to be the same as in monoculture. As
939 Ψ_{soil} represents the global pot soil water potential, it is here equal to the mean of both
940 compartment soil water potential.

941 **Figure 2.** Drought impact on water potential and hydraulic risk according to species
 942 mixture and root separation.

943

944 (A) Soil (Ψ_{soil}) and leaf predawn water potentials (Ψ_{pd}) for the different pot
 945 compositions at each measurement date. Ψ_{soil} represent average values computed at
 946 the pot level from manual weightings (grey points). The average Ψ_{pd} of *Q. ilex* and *P.*
 947 *halepensis* correspond respectively to black and white dots. Standard deviations are
 948 represented and significant differences between Ψ_{soil} and Ψ_{pd} obtained using Students'
 949 t-tests are indicated (ns, non-significant difference; *, $0.01 \leq P_{\text{value}} < 0.05$; **,
 950 $0.001 \leq P_{\text{value}} < 0.01$; ***, $P_{\text{value}} < 0.001$). For Ψ_{pd} , $N = 24$ for monocultures
 951 (pooling monocultures with and without root separation/two trees per pots) and 6 for
 952 mixtures. For Ψ_{soil} , $N = 12$ for monocultures (pooling monocultures with and without
 953 root separation) and 6 for mixtures concerning Ψ_{soil} .

954

955 (B) Hydraulic safety margins (HSM) measured at the driest date of the experiment in
 956 monocultures (with and without root separation) and the mixture without root
 957 separation. HSM were computed as the difference between Ψ_{pd} at the driest date and
 958 the P50 (i.e., Ψ_{pd} causing 50% embolism). Significant differences between HSM
 959 according species and pot modalities were obtained using Students' t-tests and are
 960 indicated (ns, non-significant difference; *, $0.01 \leq P_{\text{value}} < 0.05$). $N = 24$ for
 961 monocultures (pooling monocultures with and without root separation/two trees per
 962 pots) and 6 for mixtures. Boxes represent the median, 25th and 75th percentiles, error
 963 bars the 10th and 90th percentiles, and dots outliers.

964

965

966 **Figure 3.** Mixture effect on the hydric behavior of *Q. ilex*.

967

968 (A) Relationships between soil (Ψ_{soil}) and predawn (Ψ_{pd}) water potentials of *Q. ilex*
 969 and *P. halepensis* in mixtures with root separation, without root separation and
 970 monocultures. Different colors were used for monocultures (white dots), mixture with
 971 root separation (grey dots) and mixture without root separation (black dots). The
 972 isoline ($y=x$) is reported in orange. Distinct linear fits between Ψ_{soil} and Ψ_{pd} are
 973 depicted for significantly different relationships (see Table 2), and the corresponding
 974 equations given. For *Q. ilex*, fit between Ψ_{soil} and Ψ_{pd} combining both monoculture
 975 and mixture is represented in dashed line and in solid black line for mixture without
 976 root separation for the latter. For *P. halepensis*, fit between Ψ_{soil} and Ψ_{pd} combines all
 977 three pots modalities. $N = 96$ for monocultures (with and without root separation) and
 978 24 for mixtures for each root separation category.

979

980 (B) Relationships between predawn water potentials (Ψ_{pd}) of *Q. ilex* and *P. halepensis*
 981 in mixtures with root separation and without root separation. $N = 24$ for each root
 982 separation category. Summary statistics are shown in Table 3.

983

984 **Figure 4.** SurEau model simulations in monocultures and mixture (refer to as
 985 Benchmark simulation in the text). Upper panels show the simulated dynamics of
 986 transpiration (T_{plant} , in g/h) and the total tree transpiration until hydraulic failure
 987 (Total T_{plant} , in g). Lower panels show the leaf (Ψ_{leaf}) and soil (Ψ_{soil}) water potentials.
 988 The time to reach hydraulic failure (THF, corresponding to the number of days to
 989 reach 100% loss in hydraulic conductivity) is indicated in white and black

990 respectively for *P. halepensis* and *Q. ilex* respectively for the different composition
991 treatments.

992

993 **Figure 5.** Sensitivity analysis with the SurEau model to explore the role of K_{root} , g_{cuti}
994 and K_{soil} (which is modified through the fine root length) on the changes of the
995 relationship between soil water potential (Ψ_{soil}) and plant water potential (Ψ_{leaf}). (A)
996 Test of sensitivity to root conductance (K_{root}) and leaf cuticular conductance (g_{cuti})
997 parameters for *P. halepensis*. (B) Test of sensitivity to fine root length for *Q. ilex*
998 (fine root length multiplied by $\frac{1}{2}$, 1 and 4 compared to the benchmark). Note that the
999 scales of the x-axis differ between plots. Model parameters are provided in the Tables
1000 4 and 5.

1001

1002

1003 References

- 1004 Adams, H.D., Zeppel, M.J.B., Anderegg, W.R.L., Hartmann, H., Landh usser, S.M., Tissue,
1005 D.T., Huxman, T.E., Hudson, P.J., Franz, T.E., Allen, C.D., Anderegg, L.D.L.,
1006 Barron-Gafford, G.A., Beerling, D.J., Breshears, D.D., Brodrigg, T.J., Bugmann, H.,
1007 Cobb, R.C., Collins, A.D., Dickman, L.T., Duan, H., Ewers, B.E., Galiano, L.,
1008 Galvez, D.A., Garcia-Forner, N., Gaylord, M.L., Germino, M.J., Gessler, A., Hacke,
1009 U.G., Hakamada, R., Hector, A., Jenkins, M.W., Kane, J.M., Kolb, T.E., Law, D.J.,
1010 Lewis, J.D., Limousin, J.-M., Love, D.M., Macalady, A.K., Mart nez-Vilalta, J.,
1011 Mencuccini, M., Mitchell, P.J., Muss, J.D., O’Brien, M.J., O’Grady, A.P., Pangle,
1012 R.E., Pinkard, E.A., Piper, F.I., Plaut, J.A., Pockman, W.T., Quirk, J., Reinhardt, K.,
1013 Ripullone, F., Ryan, M.G., Sala, A., Sevanto, S., Sperry, J.S., Vargas, R., Vennetier,
1014 M., Way, D.A., Xu, C., Yezpez, E.A., McDowell, N.G., 2017. A multi-species
1015 synthesis of physiological mechanisms in drought-induced tree mortality. *Nat Ecol*
1016 *Evol* 1, 1285–1291. <https://doi.org/10.1038/s41559-017-0248-x>
- 1017 Aguad , D., Poyatos, R., Rosas, T., Mart nez-Vilalta, J., 2015. Comparative Drought
1018 Responses of *Quercus ilex* L. and *Pinus sylvestris* L. in a Montane Forest Undergoing
1019 a Vegetation Shift. *Forests* 6, 2505–2529. <https://doi.org/10.3390/f6082505>
- 1020 Allen, C.D., Macalady, A.K., Chenchouni, H., Bachelet, D., McDowell, N., Vennetier, M.,
1021 Kitzberger, T., Rigling, A., Breshears, D.D., Hogg, E.H. (Ted), Gonzalez, P.,
1022 Fensham, R., Zhang, Z., Castro, J., Demidova, N., Lim, J.-H., Allard, G., Running,
1023 S.W., Semerci, A., Cobb, N., 2010. A global overview of drought and heat-induced
1024 tree mortality reveals emerging climate change risks for forests. *Forest Ecology and*
1025 *Management, Adaptation of Forests and Forest Management to Changing Climate*
1026 259, 660–684. <https://doi.org/10.1016/j.foreco.2009.09.001>
- 1027 Anderegg, W.R.L., Konings, A.G., Trugman, A.T., Yu, K., Bowling, D.R., Gabbitas, R.,
1028 Karp, D.S., Pacala, S., Sperry, J.S., Sulman, B.N., Zenes, N., 2018. Hydraulic
1029 diversity of forests regulates ecosystem resilience during drought. *Nature* 561, 538–
1030 541. <https://doi.org/10.1038/s41586-018-0539-7>
- 1031 Archie, G.E., 1942. The Electrical Resistivity Log as an Aid in Determining Some Reservoir
1032 Characteristics. *Transactions of the AIME* 146, 54–62.
1033 <https://doi.org/10.2118/942054-G>
- 1034 Bates, D., Maechler, M., Bolker [aut, B., cre, Walker, S., Christensen, R.H.B., Singmann, H.,
1035 Dai, B., Scheipl, F., Grothendieck, G., Green, P., Fox, J., Bauer, A.,
1036 simulate.formula), P.N.K. (shared copyright on, Tanaka, E., 2023. lme4: Linear
1037 Mixed-Effects Models using “Eigen” and S4.
- 1038 Bello, J., Hasselquist, N.J., Vallet, P., Kahmen, A., Perot, T., Korboulewsky, N., 2019.
1039 Complementary water uptake depth of *Quercus petraea* and *Pinus sylvestris* in mixed

- 1040 stands during an extreme drought. *Plant Soil* 437, 93–115.
 1041 <https://doi.org/10.1007/s11104-019-03951-z>
- 1042 Billon, L.M., Blackman, C.J., Cochard, H., Badel, E., Hitmi, A., Cartailleur, J., Souchal, R.,
 1043 Torres-Ruiz, J.M., 2020. The DroughtBox: A new tool for phenotyping residual
 1044 branch conductance and its temperature dependence during drought. *Plant, Cell &*
 1045 *Environment* 43, 1584–1594. <https://doi.org/10.1111/pce.13750>
- 1046 Blanchy, G., Saneiyani, S., Boyd, J., McLachlan, P., Binley, A., 2020. ResIPy, an intuitive
 1047 open source software for complex geoelectrical inversion/modeling. *Computers &*
 1048 *Geosciences* 137, 104423. <https://doi.org/10.1016/j.cageo.2020.104423>
- 1049 Breshears, D., Adams, H., Eamus, D., McDowell, N., Law, D., Will, R., Williams, A., Zou,
 1050 C., 2013. The critical amplifying role of increasing atmospheric moisture demand on
 1051 tree mortality and associated regional die-off. *Frontiers in Plant Science* 4.
- 1052 Carsel, R.F., Parrish, R.S., 1988. Developing joint probability distributions of soil water
 1053 retention characteristics. *Water Resources Research* 24, 755–769.
 1054 <https://doi.org/10.1029/WR024i005p00755>
- 1055 Choat, B., Brodribb, T.J., Brodersen, C.R., Duursma, R.A., López, R., Medlyn, B.E., 2018.
 1056 Triggers of tree mortality under drought. *Nature* 558, 531–539.
 1057 <https://doi.org/10.1038/s41586-018-0240-x>
- 1058 Cochard, H., Pimont, F., Ruffault, J., Martin-StPaul, N., 2021. SurEau: a mechanistic model
 1059 of plant water relations under extreme drought. *Annals of Forest Science* 78, 1–23.
 1060 <https://doi.org/10.1007/s13595-021-01067-y>
- 1061 Cruziat, P., Cochard, H., Améglio, T., 2002. Hydraulic architecture of trees: main concepts
 1062 and results. *Ann. For. Sci.* 59, 723–752. <https://doi.org/10.1051/forest:2002060>
- 1063 Cuneo, I.F., Knipfer, T., Brodersen, C.R., McElrone, A.J., 2016. Mechanical Failure of Fine
 1064 Root Cortical Cells Initiates Plant Hydraulic Decline during Drought. *Plant*
 1065 *Physiology* 172, 1669–1678. <https://doi.org/10.1104/pp.16.00923>
- 1066 Dane, J.H., Topp, C.G., 2020. *Methods of Soil Analysis, Part 4: Physical Methods*. John
 1067 Wiley & Sons.
- 1068 de-Dios-García, J., Pardos, M., Calama, R., 2015. Interannual variability in competitive
 1069 effects in mixed and monospecific forests of Mediterranean stone pine. *Forest*
 1070 *Ecology and Management* 358, 230–239.
 1071 <https://doi.org/10.1016/j.foreco.2015.09.014>
- 1072 Delzon, S., 2015. New insight into leaf drought tolerance. *Functional Ecology* 29, 1247–1249.
 1073 <https://doi.org/10.1111/1365-2435.12500>
- 1074 Domec, J.-C., King, J.S., Carmichael, M.J., Overby, A.T., Wortemann, R., Smith, W.K.,
 1075 Miao, G., Noormets, A., Johnson, D.M., 2021. Aquaporins, and not changes in root
 1076 structure, provide new insights into physiological responses to drought, flooding, and
 1077 salinity. *Journal of Experimental Botany* 72, 4489–4501.
 1078 <https://doi.org/10.1093/jxb/erab100>
- 1079 Duddek, P., Carminati, A., Koebernick, N., Ohmann, L., Lovric, G., Delzon, S., Rodriguez-
 1080 Dominguez, C.M., King, A., Ahmed, M.A., 2022. The impact of drought-induced
 1081 root and root hair shrinkage on root–soil contact. *Plant Physiology* 189, 1232–1236.
 1082 <https://doi.org/10.1093/plphys/kiac144>
- 1083 Forrester, D.I., Bauhus, J., 2016. A Review of Processes Behind Diversity—Productivity
 1084 Relationships in Forests. *Curr Forestry Rep* 2, 45–61. [https://doi.org/10.1007/s40725-](https://doi.org/10.1007/s40725-016-0031-2)
 1085 [016-0031-2](https://doi.org/10.1007/s40725-016-0031-2)
- 1086 Grossiord, C., 2020. Having the right neighbors: how tree species diversity modulates drought
 1087 impacts on forests. *New Phytologist* 228, 42–49. <https://doi.org/10.1111/nph.15667>
- 1088 Grossiord, C., Gessler, A., Granier, A., Pollastrini, M., Bussotti, F., Bonal, D., 2014a.
 1089 Interspecific competition influences the response of oak transpiration to increasing
 1090 drought stress in a mixed Mediterranean forest. *Forest Ecology and Management* 318,
 1091 54–61. <https://doi.org/10.1016/j.foreco.2014.01.004>
- 1092 Grossiord, C., Granier, A., Ratcliffe, S., Bouriaud, O., Bruelheide, H., Čečko, E., Forrester,
 1093 D.I., Dawud, S.M., Finér, L., Pollastrini, M., Scherer-Lorenzen, M., Valladares, F.,
 1094 Bonal, D., Gessler, A., 2014b. Tree diversity does not always improve resistance of

- 1095 forest ecosystems to drought. *Proceedings of the National Academy of Sciences* 111,
1096 14812–14815. <https://doi.org/10.1073/pnas.1411970111>
- 1097 Grossiord, C., Sevanto, S., Bonal, D., Borrego, I., Dawson, T.E., Ryan, M., Wang, W.,
1098 McDowell, N.G., 2019. Prolonged warming and drought modify belowground
1099 interactions for water among coexisting plants. *Tree Physiology* 39, 55–63.
1100 <https://doi.org/10.1093/treephys/tpy080>
- 1101 Haberstroh, S., Werner, C., 2022. The role of species interactions for forest resilience to
1102 drought. *Plant Biology* 24, 1098–1107. <https://doi.org/10.1111/plb.13415>
- 1103 Jose, S., Williams, R., Zamora, D., 2006. Belowground ecological interactions in mixed-
1104 species forest plantations. *Forest Ecology and Management, Improving Productivity*
1105 in Mixed-Species Plantations 233, 231–239.
1106 <https://doi.org/10.1016/j.foreco.2006.05.014>
- 1107 Klein, T., 2014. The variability of stomatal sensitivity to leaf water potential across tree
1108 species indicates a continuum between isohydric and anisohydric behaviours.
1109 *Functional Ecology* 28, 1313–1320. <https://doi.org/10.1111/1365-2435.12289>
- 1110 Lebourgeois, F., Gomez, N., Pinto, P., Mérian, P., 2013. Mixed stands reduce *Abies alba* tree-
1111 ring sensitivity to summer drought in the Vosges mountains, western Europe. *Forest*
1112 *Ecology and Management* 303, 61–71. <https://doi.org/10.1016/j.foreco.2013.04.003>
- 1113 Leonova, A., Heger, A., Vásconez Navas, L.K., Jensen, K., Reisdorff, C., 2022. Fine root
1114 mortality under severe drought reflects different root distribution of *Quercus robur*
1115 and *Ulmus laevis* trees in hardwood floodplain forests. *Trees* 36, 1105–1115.
1116 <https://doi.org/10.1007/s00468-022-02275-3>
- 1117 Liu, Z., Ye, L., Jiang, J., Liu, R., Xu, Y., Jia, G., 2023. Increased uptake of deep soil water
1118 promotes drought resistance in mixed forests. *Plant, Cell & Environment* 46, 3218–
1119 3228. <https://doi.org/10.1111/pce.14642>
- 1120 López, R., Cano, F.J., Martin-StPaul, N.K., Cochard, H., Choat, B., 2021. Coordination of
1121 stem and leaf traits define different strategies to regulate water loss and tolerance
1122 ranges to aridity. *New Phytologist* 230, 497–509. <https://doi.org/10.1111/nph.17185>
- 1123 Martin-StPaul, N., Delzon, S., Cochard, H., 2017. Plant resistance to drought depends on
1124 timely stomatal closure. *Ecol Lett* 20, 1437–1447. <https://doi.org/10.1111/ele.12851>
- 1125 Mas, E., Cochard, H., Deluigi, J., Didion-Gency, M., Martin-StPaul, N., Morcillo, L.,
1126 Valladares, F., Vilagrosa, A., Grossiord, C., 2024. Interactions between beech and
1127 oak seedlings can modify the effects of hotter droughts and the onset of hydraulic
1128 failure. *New Phytologist* 241, 1021–1034. <https://doi.org/10.1111/nph.19358>
- 1129 Mencuccini, M., 2003. The ecological significance of long-distance water transport: short-
1130 term regulation, long-term acclimation and the hydraulic costs of stature across plant
1131 life forms. *Plant, Cell & Environment* 26, 163–182. <https://doi.org/10.1046/j.1365-3040.2003.00991.x>
- 1132
- 1133 Mendiburu, F. de, 2023. *agricolae: Statistical Procedures for Agricultural Research*.
- 1134 Merlin, M., Perot, T., Perret, S., Korboulewsky, N., Vallet, P., 2015. Effects of stand
1135 composition and tree size on resistance and resilience to drought in sessile oak and
1136 Scots pine. *Forest Ecology and Management* 339, 22–33.
1137 <https://doi.org/10.1016/j.foreco.2014.11.032>
- 1138 Messier, C., Bauhus, J., Sousa-Silva, R., Auge, H., Baeten, L., Barsoum, N., Bruelheide, H.,
1139 Caldwell, B., Cavender-Bares, J., Dhiedt, E., Eisenhauer, N., Ganade, G., Gravel, D.,
1140 Guillemot, J., Hall, J.S., Hector, A., Hérault, B., Jactel, H., Koricheva, J., Kreft, H.,
1141 Mereu, S., Muys, B., Nock, C.A., Paquette, A., Parker, J.D., Perring, M.P., Ponette,
1142 Q., Potvin, C., Reich, P.B., Scherer-Lorenzen, M., Schnabel, F., Verheyen, K., Weih,
1143 M., Wollni, M., Zemp, D.C., 2022. For the sake of resilience and multifunctionality,
1144 let's diversify planted forests! *Conservation Letters* 15, e12829.
1145 <https://doi.org/10.1111/conl.12829>
- 1146 Moreno, M., 2022. Influence de la plasticité phénotypique et du mélange d'espèces sur la
1147 vulnérabilité hydraulique de forêts méditerranéennes (These de doctorat). Aix-
1148 Marseille.

- 1149 Moreno, M., Simioni, G., Cailleret, M., Ruffault, J., Badel, E., Carrière, S., Davi, H., Gavinet,
1150 J., Huc, R., Limousin, J.-M., Marloie, O., Martin, L., Rodríguez-Calcerrada, J.,
1151 Vennetier, M., Martin-StPaul, N., 2021. Consistently lower sap velocity and growth
1152 over nine years of rainfall exclusion in a Mediterranean mixed pine-oak forest.
1153 *Agricultural and Forest Meteorology* 308–309, 108472.
1154 <https://doi.org/10.1016/j.agrformet.2021.108472>
- 1155 Nobel, P.S., Sanderson, J., 1984. Rectifier-like Activities of Roots of Two Desert Succulents.
1156 *Journal of Experimental Botany* 35, 727–737. <https://doi.org/10.1093/jxb/35.5.727>
- 1157 North, G.B., Nobel, P.S., 1997. Drought-induced changes in soil contact and hydraulic
1158 conductivity for roots of *Opuntia ficus-indica* with and without rhizosheaths. *Plant*
1159 *and Soil* 191, 249–258. <https://doi.org/10.1023/A:1004213728734>
- 1160 Pangle, R.E., Hill, J.P., Plaut, J.A., Yepez, E.A., Elliot, J.R., Gehres, N., McDowell, N.G.,
1161 Pockman, W.T., 2012. Methodology and performance of a rainfall manipulation
1162 experiment in a piñon–juniper woodland. *Ecosphere* 3, art28.
1163 <https://doi.org/10.1890/ES11-00369.1>
- 1164 Plaut, J.A., Yepez, E.A., Hill, J., Pangle, R., Sperry, J.S., Pockman, W.T., McDowell, N.G.,
1165 2012. Hydraulic limits preceding mortality in a piñon–juniper woodland under
1166 experimental drought. *Plant, Cell & Environment* 35, 1601–1617.
1167 <https://doi.org/10.1111/j.1365-3040.2012.02512.x>
- 1168 Rodríguez-Dominguez, C.M., Forner, A., Martorell, S., Choat, B., Lopez, R., Peters, J.M.R.,
1169 Pfautsch, S., Mayr, S., Carins-Murphy, M.R., McAdam, S.A.M., Richardson, F.,
1170 Diaz-Espejo, A., Hernandez-Santana, V., Menezes-Silva, P.E., Torres-Ruiz, J.M.,
1171 Batz, T.A., Sack, L., 2022. Leaf water potential measurements using the pressure
1172 chamber: Synthetic testing of assumptions towards best practices for precision and
1173 accuracy. *Plant, Cell & Environment* 45, 2037–2061.
1174 <https://doi.org/10.1111/pce.14330>
- 1175 Ruffault, J., Limousin, J.-M., Pimont, F., Dupuy, J.-L., De Càceres, M., Cochard, H.,
1176 Mouillot, F., Blackman, C.J., Torres-Ruiz, J.M., Parsons, R.A., Moreno, M., Delzon,
1177 S., Jansen, S., Olioso, A., Choat, B., Martin-StPaul, N., 2023. Plant hydraulic
1178 modelling of leaf and canopy fuel moisture content reveals increasing vulnerability of
1179 a Mediterranean forest to wildfires under extreme drought. *New Phytologist* 237,
1180 1256–1269. <https://doi.org/10.1111/nph.18614>
- 1181 Ruffault, J., Martin-StPaul, N., 2024. Ecophysiological and fuel moisture content data from an
1182 experimental drought study on *Pinus halepensis* and *Quercus ilex*.
1183 <https://doi.org/10.57745/JTBTF>
- 1184 Ruffault, J., Pimont, F., Cochard, H., Dupuy, J.-L., Martin-StPaul, N.K., 2022. SurEau-Ecos
1185 v2.0: A trait-based plant hydraulics model for simulations of plant water status and
1186 drought-induced mortality at the ecosystem level (preprint). *Biogeosciences*.
1187 <https://doi.org/10.5194/gmd-2022-17>
- 1188 Ruiz-Benito, P., Ratcliffe, S., Jump, A.S., Gómez-Aparicio, L., Madrigal-González, J., Wirth,
1189 C., Kändler, G., Lehtonen, A., Dahlgren, J., Kattge, J., Zavala, M.A., 2017.
1190 Functional diversity underlies demographic responses to environmental variation in
1191 European forests. *Global Ecology and Biogeography* 26, 128–141.
1192 <https://doi.org/10.1111/geb.12515>
- 1193 Sanchez-Martinez, P., Mencuccini, M., García-Valdés, R., Hammond, W.M., Serra-Diaz,
1194 J.M., Guo, W.-Y., Segovia, R.A., Dexter, K.G., Svenning, J.-C., Allen, C., Martínez-
1195 Vilalta, J., 2023. Increased hydraulic risk in assemblages of woody plant species
1196 predicts spatial patterns of drought-induced mortality. *Nat Ecol Evol* 7, 1620–1632.
1197 <https://doi.org/10.1038/s41559-023-02180-z>
- 1198 Schnabel, F., Liu, X., Kunz, M., Barry, K.E., Bongers, F.J., Bruelheide, H., Fichtner, A.,
1199 Härdtle, W., Li, S., Pfaff, C.-T., Schmid, B., Schwarz, J.A., Tang, Z., Yang, B.,
1200 Bauhus, J., von Oheimb, G., Ma, K., Wirth, C., 2021. Species richness stabilizes
1201 productivity via asynchrony and drought-tolerance diversity in a large-scale tree
1202 biodiversity experiment. *Science Advances* 7, eabk1643.
1203 <https://doi.org/10.1126/sciadv.abk1643>

- 1204 Senf, C., Buras, A., Zang, C.S., Rammig, A., Seidl, R., 2020. Excess forest mortality is
 1205 consistently linked to drought across Europe. *Nat Commun* 11, 6200.
 1206 <https://doi.org/10.1038/s41467-020-19924-1>
- 1207 Sergent, A.S., Varela, S.A., Barigah, T.S., Badel, E., Cochard, H., Dalla-Salda, G., Delzon,
 1208 S., Fernández, M.E., Guillemot, J., Gyenge, J., Lamarque, L.J., Martinez-Meier, A.,
 1209 Rozenberg, P., Torres-Ruiz, J.M., Martin-StPaul, N.K., 2020. A comparison of five
 1210 methods to assess embolism resistance in trees. *Forest Ecology and Management* 468,
 1211 118175. <https://doi.org/10.1016/j.foreco.2020.118175>
- 1212 Sun, Z., Liu, X., Schmid, B., Bruelheide, H., Bu, W., Ma, K., 2017. Positive effects of tree
 1213 species richness on fine-root production in a subtropical forest in SE-China. *Journal*
 1214 *of Plant Ecology* 10, 146–157. <https://doi.org/10.1093/jpe/rtw094>
- 1215 Ter-Mikaelian, M.T., Parker, W.C., 2000. Estimating biomass of white spruce seedlings with
 1216 vertical photo imagery. *New Forests* 20, 145–162.
 1217 <https://doi.org/10.1023/A:1006716406751>
- 1218 Trogisch, S., Liu, X., Rutten, G., Xue, K., Bauhus, J., Brose, U., Bu, W., Cesarz, S., Chesters,
 1219 D., Connolly, J., Cui, X., Eisenhauer, N., Guo, L., Haider, S., Härdtle, W., Kunz, M.,
 1220 Liu, L., Ma, Z., Neumann, S., Sang, W., Schuldt, A., Tang, Z., van Dam, N.M., von
 1221 Oheimb, G., Wang, M.-Q., Wang, S., Weinhold, A., Wirth, C., Wubet, T., Xu, X.,
 1222 Yang, B., Zhang, N., Zhu, C.-D., Ma, K., Wang, Y., Bruelheide, H., 2021. The
 1223 significance of tree-tree interactions for forest ecosystem functioning. *Basic and*
 1224 *Applied Ecology, Tree Diversity Effects on Ecosystem Functioning* 55, 33–52.
 1225 <https://doi.org/10.1016/j.baae.2021.02.003>
- 1226 Tyree, M.T., Ewers, F.W., 1991. The hydraulic architecture of trees and other woody plants.
 1227 *New Phytologist* 119, 345–360. <https://doi.org/10.1111/j.1469-8137.1991.tb00035.x>
- 1228 Tyree, M.T., Sperry, J.S., 1989. Vulnerability of Xylem to Cavitation and Embolism. *Annual*
 1229 *Review of Plant Physiology and Plant Molecular Biology* 40, 19–36.
 1230 <https://doi.org/10.1146/annurev.pp.40.060189.000315>
- 1231 van Genuchten, M.Th., 1980. A Closed-form Equation for Predicting the Hydraulic
 1232 Conductivity of Unsaturated Soils. *Soil Science Society of America Journal* 44, 892–
 1233 898. <https://doi.org/10.2136/sssaj1980.03615995004400050002x>
- 1234 Vitali, V., Forrester, D.I., Bauhus, J., 2018. Know Your Neighbours: Drought Response of
 1235 Norway Spruce, Silver Fir and Douglas Fir in Mixed Forests Depends on Species
 1236 Identity and Diversity of Tree Neighbourhoods. *Ecosystems* 21, 1215–1229.
 1237 <https://doi.org/10.1007/s10021-017-0214-0>
- 1238 Wambsgans, J., Beyer, F., Freschet, G.T., Scherer-Lorenzen, M., Bauhus, J., 2021. Tree
 1239 species mixing reduces biomass but increases length of absorptive fine roots in
 1240 European forests. *Journal of Ecology* 109, 2678–2691. <https://doi.org/10.1111/1365-2745.13675>
- 1242 Waxman, M.H., Smits, L.J.M., 1968. Electrical Conductivities in Oil-Bearing Shaly Sands.
 1243 *Society of Petroleum Engineers Journal* 8, 107–122. <https://doi.org/10.2118/1863-A>

1249 **Competing Interest Statement**

1250 Authors declare no competing interest.

1251
 1252

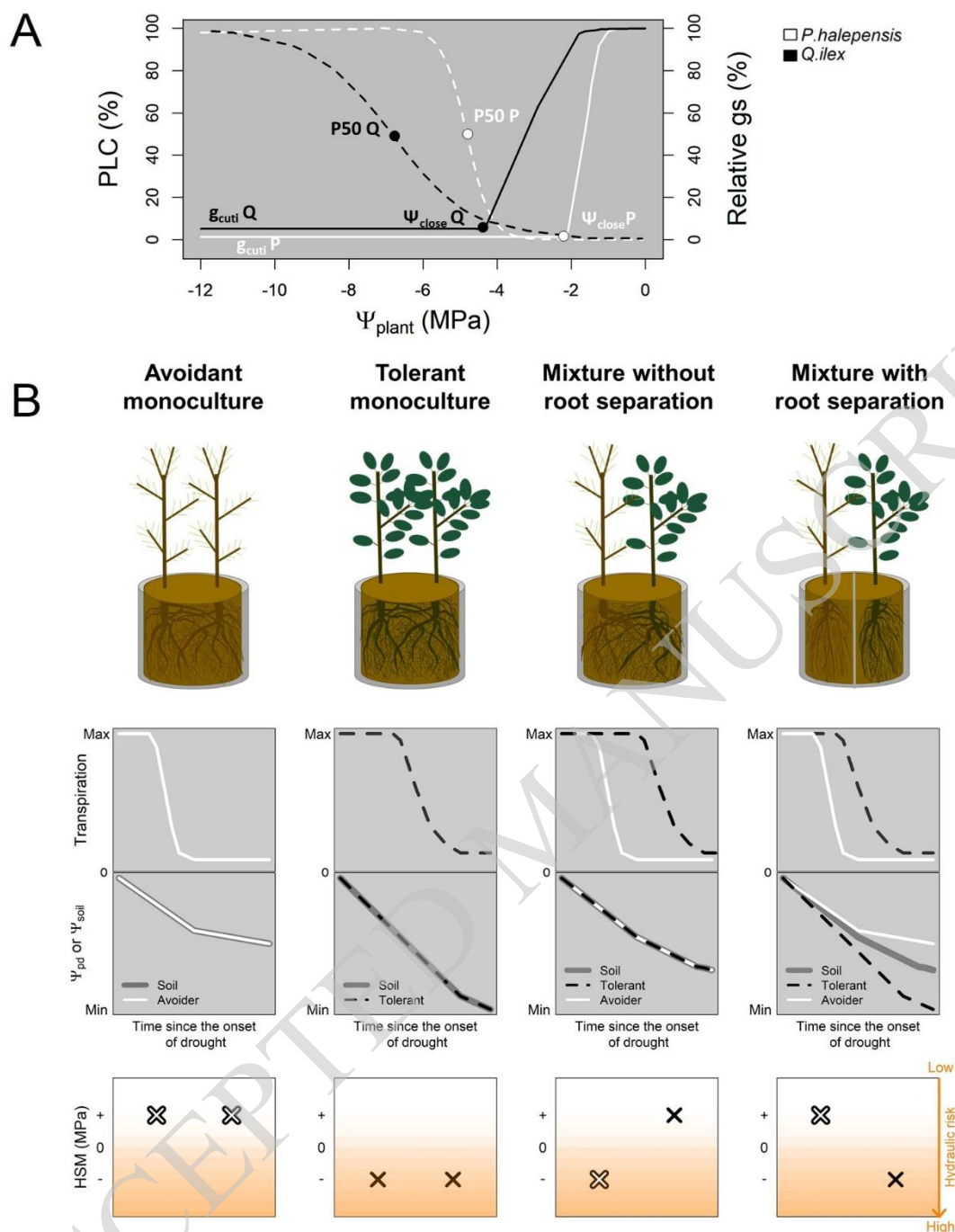


Figure 1. Conceptual representation of drought effects on hydraulic risk of monocultures and mixtures, for two species with contrasting water use strategies.

(A) Drought responses of species according the resistance strategy they adopt. During drought, the *isohydric* species (i.e., *Pinus halepensis*, also referred as drought avoidant) close its stomata at a relatively high-water potential (Ψ_{close} , corresponding to the water potential inducing full stomatal closure) and has a low cuticular conductance (g_{cuti}). Also, it has a relatively high P50 (water potential causing 50 % loss of hydraulic conductivity), making it more vulnerable to xylem cavitation. Whereas, the *anisohydric* species (i.e., *Quercus ilex*, also referred as drought tolerant), has a lower Ψ_{close} and a higher g_{cuti} , making it consuming

more water. Additionally, it has a lower P50 (water potential causing 50 % loss of hydraulic conductivity), making it more resistant to xylem cavitation.

(B) Experimental design and hypothesized drought responses for monocultures and mixtures of an *isohydric* (drought avoidant) and an *anisohydric* (drought tolerant) species. The transpiration, water potentials (Ψ_{soil} : overall pot soil water potential; Ψ_{pd} : plant predawn water potential) and hydraulic safety margins (HSM) for each situation and species. HSM represents the risk of hydraulic failure, it generally refers as the difference between the minimum plant water potential and vulnerability to cavitation (P50, the water potential causing 50 % of embolism). In the *isohydric* monoculture, tree transpiration is expected to reduce rapidly after the onset of drought, limiting the drop in Ψ_{soil} and Ψ_{pd} , and hence the hydraulic failure risk (positive HSM). In the *anisohydric* monoculture, transpiration should decrease later as stomatal control is expected to be more released than the one of the *isohydric* species. This should trigger a steeper decrease of Ψ_{soil} and Ψ_{pd} , thereby increasing the risk of hydraulic failure (more negative HSM). In the mixture without root separation, transpiration of the *isohydric* should decrease earlier than for the *anisohydric*. This is expected to dampen overall soil water loss and thus Ψ_{pd} and HSM of the *anisohydric* species compared to the monoculture. However, the water consumption of the *anisohydric* continue beyond the point of stomatal closure and of cavitation of the *isohydric*. This triggers a decrease of steeper decline of Ψ_{pd} and HSM for the *isohydric* compare to monoculture. A mixture with root separation illustrates that when each species root system occupies its proper soil volume, the regulation of the transpiration, the water potentials dynamics and the HSM are expected to be the same as in monoculture. As Ψ_{soil} represents the global pot soil water potential, it is here equal to the mean of both compartment soil water potential.

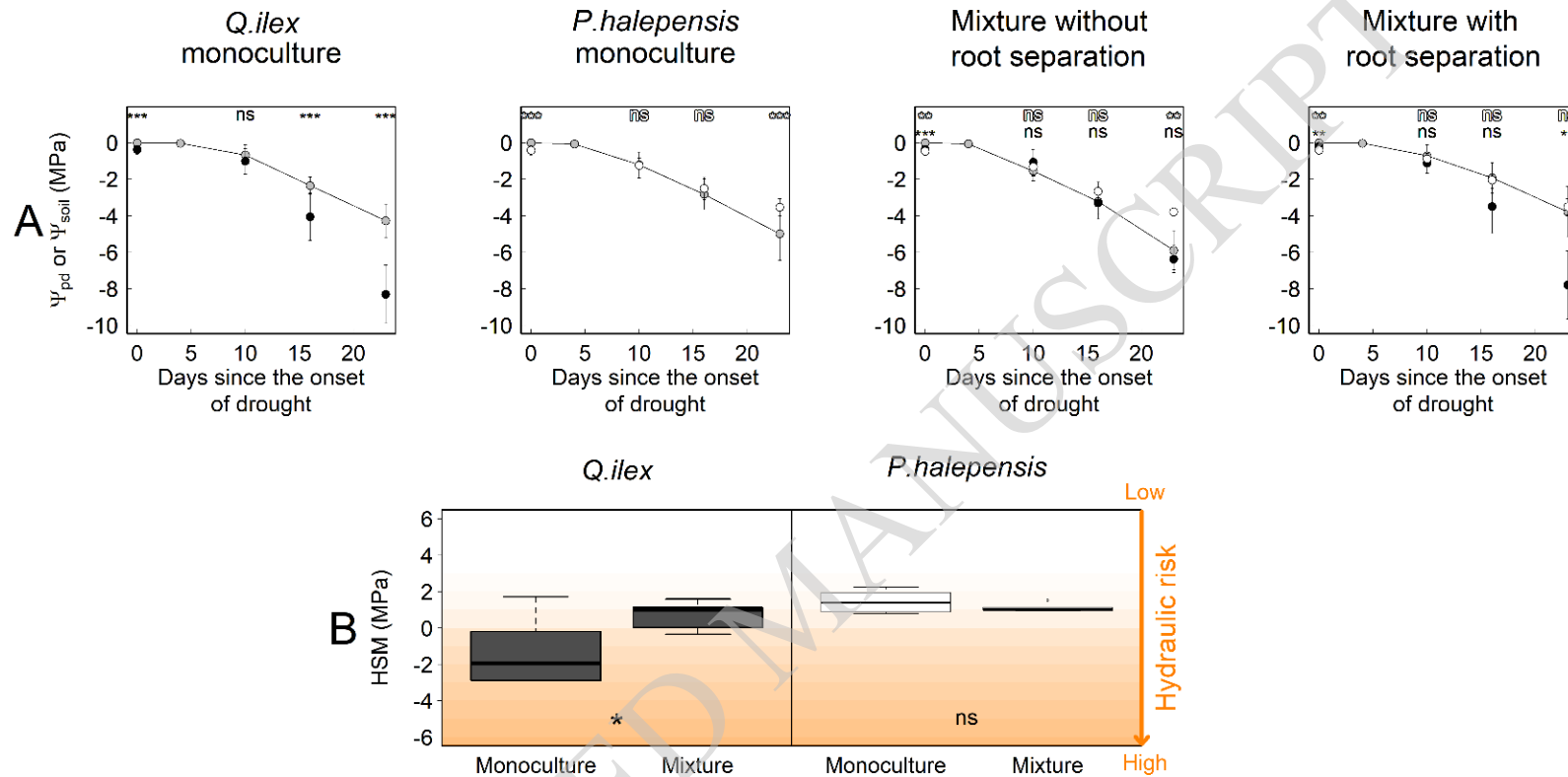


Figure 2. Drought impact on water potential and hydraulic risk according to species mixture and root separation.

(A) Soil (Ψ_{soil}) and leaf predawn water potentials (Ψ_{pd}) for the different pot compositions at each measurement date. Ψ_{soil} represent average values computed at the pot level from manual weightings (grey points). The average Ψ_{pd} of *Q. ilex* and *P. halepensis* correspond respectively to black and white dots. Standard deviations are represented and significant differences between Ψ_{soil} and Ψ_{pd} obtained using Students' t-tests are indicated (ns, non-significant difference; *, $0.01 \leq P_value < 0.05$; **, $0.001 \leq P_value < 0.01$; ***, $P_value < 0.001$). For Ψ_{pd} , $N = 24$ for

monocultures (pooling monocultures with and without root separation/two trees per pots) and 6 for mixtures. For Ψ_{soil} , $N = 12$ for monocultures (pooling monocultures with and without root separation) and 6 for mixtures concerning Ψ_{soil} .

(B) Hydraulic safety margins (HSM) measured at the driest date of the experiment in monocultures (with and without root separation) and the mixture without root separation. HSM were computed as the difference between Ψ_{pd} at the driest date and the P50 (i.e., Ψ_{pd} causing 50% embolism). Significant differences between HSM according species and pot modalities were obtained using Students' t-tests and are indicated (ns, non-significant difference; *, $0.01 \leq P_{\text{value}} < 0.05$). $N = 24$ for monocultures (pooling monocultures with and without root separation/two trees per pots) and 6 for mixtures. Boxes represent the median, 25th and 75th percentiles, error bars the 10th and 90th percentiles, and dots outliers.

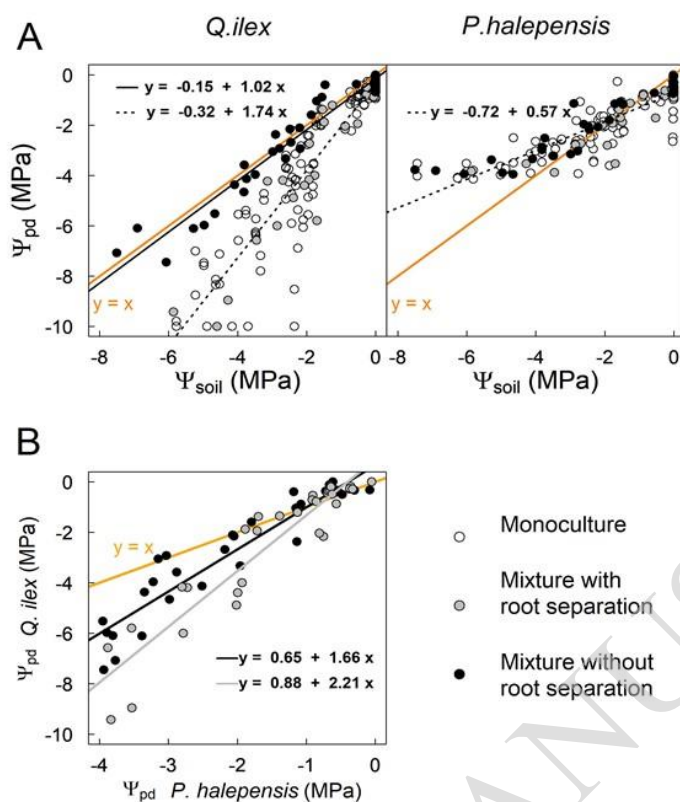


Figure 3. Mixture effect on the hydric behavior of *Q. ilex*.

(A) Relationships between soil (Ψ_{soil}) and predawn (Ψ_{pd}) water potentials of *Q. ilex* and *P. halepensis* in mixtures with root separation, without root separation and monocultures. Different colors were used for monocultures (white dots), mixture with root separation (grey dots) and mixture without root separation (black dots). The isoline ($y=x$) is reported in orange. Distinct linear fits between Ψ_{soil} and Ψ_{pd} are depicted for significantly different relationships (see Table 2), and the corresponding equations given. For *Q. ilex*, fit between Ψ_{soil} and Ψ_{pd} combining both monoculture and mixture is represented in dashed line and in solid black line for mixture without root separation for the latter. For *P. halepensis*, fit between Ψ_{soil} and Ψ_{pd} combines all three pots modalities. $N = 96$ for monocultures (with and without root separation) and 24 for mixtures for each root separation category.

(B) Relationships between predawn water potentials (Ψ_{pd}) of *Q. ilex* and *P. halepensis* in mixtures with root separation and without root separation. $N = 24$ for each root separation category. Summary statistics are shown in Table 3.

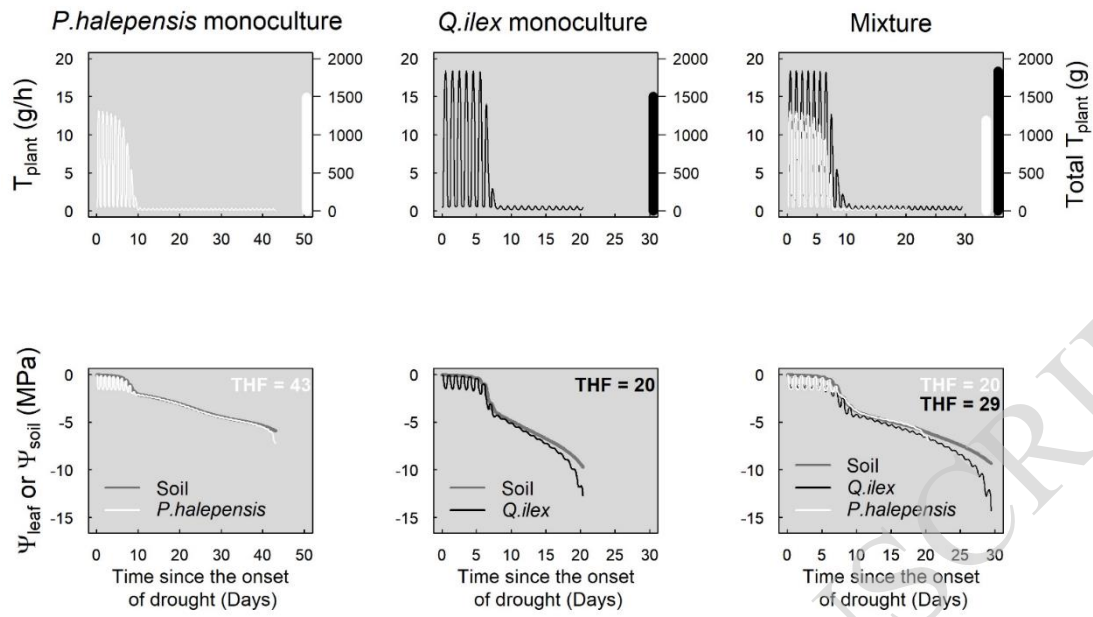


Figure 4. SurEau model simulations in monocultures and mixture (refer to as Benchmark simulation in the text). Upper panels show the simulated dynamics of transpiration (T_{plant} , in g/h) and the total tree transpiration until hydraulic failure (Total T_{plant} , in g). Lower panels show the leaf (Ψ_{leaf}) and soil (Ψ_{soil}) water potentials. The time to reach hydraulic failure (THF, corresponding to the number of days to reach 100% loss in hydraulic conductivity) is indicated in white and black respectively for *P. halepensis* and *Q. ilex* respectively for the different composition treatments.

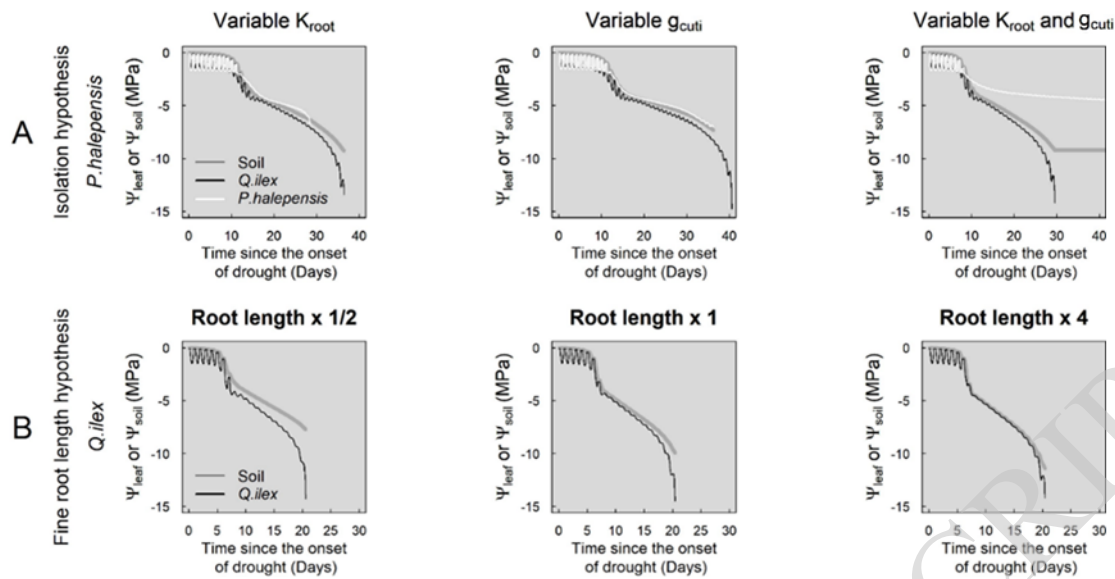


Figure 5. Sensitivity analysis with the SurEau model to explore the role of K_{root} , g_{cuti} and K_{soil} (which is modified through the fine root length) on the changes of the relationship between soil water potential (Ψ_{soil}) and plant water potential (Ψ_{leaf}). (A) Test of sensitivity to root conductance (K_{root}) and leaf cuticular conductance (g_{cuti}) parameters for *P. halepensis*. (B) Test of sensitivity to fine root length for *Q. ilex* (fine root length multiplied by $\frac{1}{2}$, 1 and 4 compared to the benchmark). Note that the scales of the x-axis differ between plots. Model parameters are provided in the Tables 4 and 5.

Parsed Citations

Adams, H.D., Zeppel, M.J.B., Anderegg, W.R.L., Hartmann, H., Landhäusser, S.M., Tissue, D.T., Huxman, T.E., Hudson, P.J., Franz, T.E., Allen, C.D., Anderegg, L.D.L., Barron-Gafford, G.A., Beerling, D.J., Breshears, D.D., Brodribb, T.J., Bugmann, H., Cobb, R.C., Collins, A.D., Dickman, L.T., Duan, H., Ewers, B.E., Galiano, L., Galvez, D.A., Garcia-Forner, N., Gaylord, M.L., Germino, M.J., Gessler, A., Hacke, U.G., Hakamada, R., Hector, A., Jenkins, M.W., Kane, J.M., Kolb, T.E., Law, D.J., Lewis, J.D., Limousin, J.-M., Love, D.M., Macalady, A.K., Martínez-Vilalta, J., Mencuccini, M., Mitchell, P.J., Muss, J.D., O'Brien, M.J., O'Grady, A.P., Pangle, R.E., Pinkard, E.A., Piper, F.I., Plaut, J.A., Pockman, W.T., Quirk, J., Reinhardt, K., Ripullone, F., Ryan, M.G., Sala, A., Sevanto, S., Sperry, J.S., Vargas, R., Vennetier, M., Way, D.A., Xu, C., Yezzer, E.A., McDowell, N.G., 2017. A multi-species synthesis of physiological mechanisms in drought-induced tree mortality. *Nat Ecol Evol* 1, 1285–1291. <https://doi.org/10.1038/s41559-017-0248-x>

Google Scholar: [Author Only](#) [Title Only](#) [Author and Title](#)

Aguadé, D., Poyatos, R., Rosas, T., Martínez-Vilalta, J., 2015. Comparative Drought Responses of *Quercus ilex* L. and *Pinus sylvestris* L. in a Montane Forest Undergoing a Vegetation Shift. *Forests* 6, 2505–2529. <https://doi.org/10.3390/f6082505>

Google Scholar: [Author Only](#) [Title Only](#) [Author and Title](#)

Allen, C.D., Macalady, A.K., Chenchouni, H., Bachelet, D., McDowell, N., Vennetier, M., Kitzberger, T., Rigling, A., Breshears, D.D., Hogg, E.H. (Ted), Gonzalez, P., Fensham, R., Zhang, Z., Castro, J., Demidova, N., Lim, J.-H., Allard, G., Running, S.W., Semerci, A., Cobb, N., 2010. A global overview of drought and heat-induced tree mortality reveals emerging climate change risks for forests. *Forest Ecology and Management, Adaptation of Forests and Forest Management to Changing Climate* 259, 660–684. <https://doi.org/10.1016/j.foreco.2009.09.001>

Google Scholar: [Author Only](#) [Title Only](#) [Author and Title](#)

Anderegg, W.R.L., Konings, A.G., Trugman, A.T., Yu, K., Bowling, D.R., Gabbitas, R., Karp, D.S., Pacala, S., Sperry, J.S., Sulman, B.N., Zenes, N., 2018. Hydraulic diversity of forests regulates ecosystem resilience during drought. *Nature* 561, 538–541. <https://doi.org/10.1038/s41586-018-0539-7>

Google Scholar: [Author Only](#) [Title Only](#) [Author and Title](#)

Archie, G.E., 1942. The Electrical Resistivity Log as an Aid in Determining Some Reservoir Characteristics. *Transactions of the AIME* 146, 54–62. <https://doi.org/10.2118/942054-G>

Google Scholar: [Author Only](#) [Title Only](#) [Author and Title](#)

Bates, D., Maechler, M., Bolker [aut, B., cre, Walker, S., Christensen, R.H.B., Singmann, H., Dai, B., Scheipl, F., Grothendieck, G., Green, P., Fox, J., Bauer, A., simulate.formula), P.N.K. (shared copyright on, Tanaka, E., 2023. lme4: Linear Mixed-Effects Models using "Eigen" and S4.

Google Scholar: [Author Only](#) [Title Only](#) [Author and Title](#)

Bello, J., Hasselquist, N.J., Vallet, P., Kahmen, A., Perot, T., Korboulewsky, N., 2019. Complementary water uptake depth of *Quercus petraea* and *Pinus sylvestris* in mixed stands during an extreme drought. *Plant Soil* 437, 93–115. <https://doi.org/10.1007/s11104-019-03951-z>

Google Scholar: [Author Only](#) [Title Only](#) [Author and Title](#)

Billon, L.M., Blackman, C.J., Cochard, H., Badel, E., Hitmi, A., Cartailier, J., Souchal, R., Torres-Ruiz, J.M., 2020. The DroughtBox: A new tool for phenotyping residual branch conductance and its temperature dependence during drought. *Plant, Cell & Environment* 43, 1584–1594. <https://doi.org/10.1111/pce.13750>

Google Scholar: [Author Only](#) [Title Only](#) [Author and Title](#)

Blanchy, G., Saneiyan, S., Boyd, J., McLachlan, P., Binley, A., 2020. ResIPy, an intuitive open source software for complex geoelectrical inversion/modeling. *Computers & Geosciences* 137, 104423. <https://doi.org/10.1016/j.cageo.2020.104423>

Google Scholar: [Author Only](#) [Title Only](#) [Author and Title](#)

Breshears, D., Adams, H., Earnus, D., McDowell, N., Law, D., Will, R., Williams, A., Zou, C., 2013. The critical amplifying role of increasing atmospheric moisture demand on tree mortality and associated regional die-off. *Frontiers in Plant Science* 4.

Google Scholar: [Author Only](#) [Title Only](#) [Author and Title](#)

Carsel, R.F., Parrish, R.S., 1988. Developing joint probability distributions of soil water retention characteristics. *Water Resources Research* 24, 755–769. <https://doi.org/10.1029/WR024i005p00755>

Google Scholar: [Author Only](#) [Title Only](#) [Author and Title](#)

Choat, B., Brodribb, T.J., Brodersen, C.R., Duursma, R.A., López, R., Medlyn, B.E., 2018. Triggers of tree mortality under drought. *Nature* 558, 531–539. <https://doi.org/10.1038/s41586-018-0240-x>

Google Scholar: [Author Only](#) [Title Only](#) [Author and Title](#)

Cochard, H., Pimont, F., Ruffault, J., Martin-StPaul, N., 2021. SurEau: a mechanistic model of plant water relations under extreme drought. *Annals of Forest Science* 78, 1–23. <https://doi.org/10.1007/s13595-021-01067-y>

Google Scholar: [Author Only](#) [Title Only](#) [Author and Title](#)

Cruziat, P., Cochard, H., Améglio, T., 2002. Hydraulic architecture of trees: main concepts and results. *Ann. For. Sci.* 59, 723–752. <https://doi.org/10.1051/forest:2002060>

Google Scholar: [Author Only](#) [Title Only](#) [Author and Title](#)

Cuneo, I.F., Knipfer, T., Brodersen, C.R., McElrone, A.J., 2016. Mechanical Failure of Fine Root Cortical Cells Initiates Plant Hydraulic Decline during Drought. *Plant Physiology* 172, 1669–1678. <https://doi.org/10.1104/pp.16.00923>

Google Scholar: [Author Only](#) [Title Only](#) [Author and Title](#)

Dane, J.H., Topp, C.G., 2020. *Methods of Soil Analysis, Part 4: Physical Methods*. John Wiley & Sons.

Google Scholar: [Author Only](#) [Title Only](#) [Author and Title](#)

de-Dios-García, J., Pardos, M., Calama, R., 2015. Interannual variability in competitive effects in mixed and monospecific forests of Mediterranean stone pine. *Forest Ecology and Management* 358, 230–239. <https://doi.org/10.1016/j.foreco.2015.09.014>

Google Scholar: [Author Only](#) [Title Only](#) [Author and Title](#)

Delzon, S., 2015. New insight into leaf drought tolerance. *Functional Ecology* 29, 1247–1249. <https://doi.org/10.1111/1365-2435.12500>

Google Scholar: [Author Only](#) [Title Only](#) [Author and Title](#)

Domec, J.-C., King, J.S., Carmichael, M.J., Overby, A.T., Wortemann, R., Smith, W.K., Miao, G., Noormets, A., Johnson, D.M., 2021. Aquaporins, and not changes in root structure, provide new insights into physiological responses to drought, flooding, and salinity. *Journal of Experimental Botany* 72, 4489–4501. <https://doi.org/10.1093/jxb/erab100>

Google Scholar: [Author Only](#) [Title Only](#) [Author and Title](#)

Duddek, P., Carminati, A., Koebernick, N., Ohmann, L., Lovric, G., Delzon, S., Rodriguez-Dominguez, C.M., King, A., Ahmed, M.A., 2022. The impact of drought-induced root and root hair shrinkage on root–soil contact. *Plant Physiology* 189, 1232–1236. <https://doi.org/10.1093/plphys/kiac144>

Google Scholar: [Author Only](#) [Title Only](#) [Author and Title](#)

Forrester, D.I., Bauhus, J., 2016. A Review of Processes Behind Diversity-Productivity Relationships in Forests. *Curr Forestry Rep* 2, 45–61. <https://doi.org/10.1007/s40725-016-0031-2>

Google Scholar: [Author Only](#) [Title Only](#) [Author and Title](#)

Grossiord, C., 2020. Having the right neighbors: how tree species diversity modulates drought impacts on forests. *New Phytologist* 228, 42–49. <https://doi.org/10.1111/nph.15667>

Google Scholar: [Author Only](#) [Title Only](#) [Author and Title](#)

Grossiord, C., Gessler, A., Granier, A., Pollastrini, M., Bussotti, F., Bonal, D., 2014a. Interspecific competition influences the response of oak transpiration to increasing drought stress in a mixed Mediterranean forest. *Forest Ecology and Management* 318, 54–61. <https://doi.org/10.1016/j.foreco.2014.01.004>

Google Scholar: [Author Only](#) [Title Only](#) [Author and Title](#)

Grossiord, C., Granier, A., Ratcliffe, S., Bouriaud, O., Bruehlheide, H., Češko, E., Forrester, D.I., Dawud, S.M., Finér, L., Pollastrini, M., Scherer-Lorenzen, M., Valladares, F., Bonal, D., Gessler, A., 2014b. Tree diversity does not always improve resistance of forest ecosystems to drought. *Proceedings of the National Academy of Sciences* 111, 14812–14815. <https://doi.org/10.1073/pnas.1411970111>

Google Scholar: [Author Only](#) [Title Only](#) [Author and Title](#)

Grossiord, C., Sevanto, S., Bonal, D., Borrego, I., Dawson, T.E., Ryan, M., Wang, W., McDowell, N.G., 2019. Prolonged warming and drought modify belowground interactions for water among coexisting plants. *Tree Physiology* 39, 55–63. <https://doi.org/10.1093/treephys/tpy080>

Google Scholar: [Author Only](#) [Title Only](#) [Author and Title](#)

Haberstroh, S., Werner, C., 2022. The role of species interactions for forest resilience to drought. *Plant Biology* 24, 1098–1107. <https://doi.org/10.1111/plb.13415>

Google Scholar: [Author Only](#) [Title Only](#) [Author and Title](#)

Jose, S., Williams, R., Zamora, D., 2006. Belowground ecological interactions in mixed-species forest plantations. *Forest Ecology and Management, Improving Productivity in Mixed-Species Plantations* 233, 231–239. <https://doi.org/10.1016/j.foreco.2006.05.014>

Google Scholar: [Author Only](#) [Title Only](#) [Author and Title](#)

Klein, T., 2014. The variability of stomatal sensitivity to leaf water potential across tree species indicates a continuum between isohydric and anisohydric behaviours. *Functional Ecology* 28, 1313–1320. <https://doi.org/10.1111/1365-2435.12289>

Google Scholar: [Author Only](#) [Title Only](#) [Author and Title](#)

Lebourgeois, F., Gomez, N., Pinto, P., Mérian, P., 2013. Mixed stands reduce *Abies alba* tree-ring sensitivity to summer drought in the Vosges mountains, western Europe. *Forest Ecology and Management* 303, 61–71. <https://doi.org/10.1016/j.foreco.2013.04.003>

Google Scholar: [Author Only](#) [Title Only](#) [Author and Title](#)

Leonova, A., Heger, A., Váscónez Navas, L.K., Jensen, K., Reisdorff, C., 2022. Fine root mortality under severe drought reflects different root distribution of *Quercus robur* and *Ulmus laevis* trees in hardwood floodplain forests. *Trees* 36, 1105–1115. <https://doi.org/10.1007/s00468-022-02275-3>

Google Scholar: [Author Only Title Only Author and Title](#)

Liu, Z., Ye, L., Jiang, J., Liu, R., Xu, Y., Jia, G., 2023. Increased uptake of deep soil water promotes drought resistance in mixed forests. *Plant, Cell & Environment* 46, 3218–3228. <https://doi.org/10.1111/pce.14642>

Google Scholar: [Author Only Title Only Author and Title](#)

López, R., Cano, F.J., Martin-StPaul, N.K., Cochard, H., Choat, B., 2021. Coordination of stem and leaf traits define different strategies to regulate water loss and tolerance ranges to aridity. *New Phytologist* 230, 497–509. <https://doi.org/10.1111/nph.17185>

Google Scholar: [Author Only Title Only Author and Title](#)

Martin-StPaul, N., Delzon, S., Cochard, H., 2017. Plant resistance to drought depends on timely stomatal closure. *Ecol Lett* 20, 1437–1447. <https://doi.org/10.1111/ele.12851>

Google Scholar: [Author Only Title Only Author and Title](#)

Mas, E., Cochard, H., Deluigi, J., Didion-Gency, M., Martin-StPaul, N., Morcillo, L., Valladares, F., Vilagrosa, A., Grossiord, C., 2024. Interactions between beech and oak seedlings can modify the effects of hotter droughts and the onset of hydraulic failure. *New Phytologist* 241, 1021–1034. <https://doi.org/10.1111/nph.19358>

Google Scholar: [Author Only Title Only Author and Title](#)

Mencuccini, M., 2003. The ecological significance of long-distance water transport: short-term regulation, long-term acclimation and the hydraulic costs of stature across plant life forms. *Plant, Cell & Environment* 26, 163–182. <https://doi.org/10.1046/j.1365-3040.2003.00991.x>

Google Scholar: [Author Only Title Only Author and Title](#)

Mendiburu, F. de, 2023. agricolae: Statistical Procedures for Agricultural Research.

Merlin, M., Perot, T., Perret, S., Korboulewsky, N., Vallet, P., 2015. Effects of stand composition and tree size on resistance and resilience to drought in sessile oak and Scots pine. *Forest Ecology and Management* 339, 22–33. <https://doi.org/10.1016/j.foreco.2014.11.032>

Google Scholar: [Author Only Title Only Author and Title](#)

Messier, C., Bauhus, J., Sousa-Silva, R., Auge, H., Baeten, L., Barsoum, N., Bruelheide, H., Caldwell, B., Cavender-Bares, J., Dhiedt, E., Eisenhauer, N., Ganade, G., Gravel, D., Guillemot, J., Hall, J.S., Hector, A., Hérault, B., Jactel, H., Koricheva, J., Kreft, H., Mereu, S., Muys, B., Nock, C.A., Paquette, A., Parker, J.D., Perring, M.P., Ponette, Q., Potvin, C., Reich, P.B., Scherer-Lorenzen, M., Schnabel, F., Verheyen, K., Weih, M., Wollni, M., Zemp, D.C., 2022. For the sake of resilience and multifunctionality, let's diversify planted forests! *Conservation Letters* 15, e12829. <https://doi.org/10.1111/conl.12829>

Google Scholar: [Author Only Title Only Author and Title](#)

Moreno, M., 2022. Influence de la plasticité phénotypique et du mélange d'espèces sur la vulnérabilité hydraulique de forêts méditerranéennes (These de doctorat). Aix-Marseille.

Google Scholar: [Author Only Title Only Author and Title](#)

Moreno, M., Simioni, G., Cailleret, M., Ruffault, J., Badel, E., Carrière, S., Davi, H., Gavinet, J., Huc, R., Limousin, J.-M., Marloie, O., Martin, L., Rodríguez-Calcerrada, J., Vennetier, M., Martin-StPaul, N., 2021. Consistently lower sap velocity and growth over nine years of rainfall exclusion in a Mediterranean mixed pine-oak forest. *Agricultural and Forest Meteorology* 308–309, 108472. <https://doi.org/10.1016/j.agrformet.2021.108472>

Google Scholar: [Author Only Title Only Author and Title](#)

Nobel, P.S., Sanderson, J., 1984. Rectifier-like Activities of Roots of Two Desert Succulents. *Journal of Experimental Botany* 35, 727–737. <https://doi.org/10.1093/jxb/35.5.727>

Google Scholar: [Author Only Title Only Author and Title](#)

North, G.B., Nobel, P.S., 1997. Drought-induced changes in soil contact and hydraulic conductivity for roots of *Opuntia ficus-indica* with and without rhizosheaths. *Plant and Soil* 191, 249–258. <https://doi.org/10.1023/A:1004213728734>

Google Scholar: [Author Only Title Only Author and Title](#)

Pangle, R.E., Hill, J.P., Plaut, J.A., Yezpez, E.A., Elliot, J.R., Gehres, N., McDowell, N.G., Pockman, W.T., 2012. Methodology and performance of a rainfall manipulation experiment in a piñon–juniper woodland. *Ecosphere* 3, art28. <https://doi.org/10.1890/ES11-00369.1>

Google Scholar: [Author Only Title Only Author and Title](#)

Plaut, J.A., Yezpez, E.A., Hill, J., Pangle, R., Sperry, J.S., Pockman, W.T., McDowell, N.G., 2012. Hydraulic limits preceding mortality in a piñon–juniper woodland under experimental drought. *Plant, Cell & Environment* 35, 1601–1617. <https://doi.org/10.1111/j.1365-3040.2012.02512.x>

Google Scholar: [Author Only Title Only Author and Title](#)

Rodríguez-Domínguez, C.M., Forner, A., Martorell, S., Choat, B., Lopez, R., Peters, J.M.R., Pfautsch, S., Mayr, S., Carins-Murphy, M.R., McAdam, S.A.M., Richardson, F., Diaz-Espejo, A., Hernandez-Santana, V., Menezes-Silva, P.E., Torres-Ruiz, J.M., Batz, T.A., Sack, L., 2022. Leaf water potential measurements using the pressure chamber: Synthetic testing of assumptions towards best practices for precision and accuracy. *Plant, Cell & Environment* 45, 2037–2061. <https://doi.org/10.1111/pce.14330>

Google Scholar: [Author Only](#) [Title Only](#) [Author and Title](#)

Ruffault, J., Limousin, J.-M., Pimont, F., Dupuy, J.-L., De Càceres, M., Cochard, H., Mouillot, F., Blackman, C.J., Torres-Ruiz, J.M., Parsons, R.A., Moreno, M., Delzon, S., Jansen, S., Olioso, A., Choat, B., Martin-StPaul, N., 2023. Plant hydraulic modelling of leaf and canopy fuel moisture content reveals increasing vulnerability of a Mediterranean forest to wildfires under extreme drought. *New Phytologist* 237, 1256–1269. <https://doi.org/10.1111/nph.18614>

Google Scholar: [Author Only](#) [Title Only](#) [Author and Title](#)

Ruffault, J., Martin-StPaul, N., 2024. Ecophysiological and fuel moisture content data from an experimental drought study on *Pinus halepensis* and *Quercus ilex*. <https://doi.org/10.57745/JTBTF>

Google Scholar: [Author Only](#) [Title Only](#) [Author and Title](#)

Ruffault, J., Pimont, F., Cochard, H., Dupuy, J.-L., Martin-StPaul, N.K., 2022. SurEau-Ecos v2.0: A trait-based plant hydraulics model for simulations of plant water status and drought-induced mortality at the ecosystem level (preprint). *Biogeosciences*. <https://doi.org/10.5194/gmd-2022-17>

Google Scholar: [Author Only](#) [Title Only](#) [Author and Title](#)

Ruiz-Benito, P., Ratcliffe, S., Jump, A.S., Gómez-Aparicio, L., Madrigal-González, J., Wirth, C., Kändler, G., Lehtonen, A., Dahlgren, J., Kattge, J., Zavala, M.A., 2017. Functional diversity underlies demographic responses to environmental variation in European forests. *Global Ecology and Biogeography* 26, 128–141. <https://doi.org/10.1111/geb.12515>

Google Scholar: [Author Only](#) [Title Only](#) [Author and Title](#)

Sanchez-Martinez, P., Mencuccini, M., García-Valdés, R., Hammond, W.M., Serra-Diaz, J.M., Guo, W.-Y., Segovia, R.A., Dexter, K.G., Svenning, J.-C., Allen, C., Martínez-Vilalta, J., 2023. Increased hydraulic risk in assemblages of woody plant species predicts spatial patterns of drought-induced mortality. *Nat Ecol Evol* 7, 1620–1632. <https://doi.org/10.1038/s41559-023-02180-z>

Google Scholar: [Author Only](#) [Title Only](#) [Author and Title](#)

Schnabel, F., Liu, X., Kunz, M., Barry, K.E., Bongers, F.J., Bruelheide, H., Fichtner, A., Härdtle, W., Li, S., Pfaff, C.-T., Schmid, B., Schwarz, J.A., Tang, Z., Yang, B., Bauhus, J., von Oheimb, G., Ma, K., Wirth, C., 2021. Species richness stabilizes productivity via asynchrony and drought-tolerance diversity in a large-scale tree biodiversity experiment. *Science Advances* 7, eabk1643. <https://doi.org/10.1126/sciadv.abk1643>

Google Scholar: [Author Only](#) [Title Only](#) [Author and Title](#)

Senf, C., Buras, A., Zang, C.S., Rammig, A., Seidl, R., 2020. Excess forest mortality is consistently linked to drought across Europe. *Nat Commun* 11, 6200. <https://doi.org/10.1038/s41467-020-19924-1>

Google Scholar: [Author Only](#) [Title Only](#) [Author and Title](#)

Sergent, A.S., Varela, S.A., Barigah, T.S., Badel, E., Cochard, H., Dalla-Salda, G., Delzon, S., Fernández, M.E., Guillemot, J., Gyenge, J., Lamarque, L.J., Martinez-Meier, A., Rozenberg, P., Torres-Ruiz, J.M., Martin-StPaul, N.K., 2020. A comparison of five methods to assess embolism resistance in trees. *Forest Ecology and Management* 468, 118175. <https://doi.org/10.1016/j.foreco.2020.118175>

Google Scholar: [Author Only](#) [Title Only](#) [Author and Title](#)

Sun, Z., Liu, X., Schmid, B., Bruelheide, H., Bu, W., Ma, K., 2017. Positive effects of tree species richness on fine-root production in a subtropical forest in SE-China. *Journal of Plant Ecology* 10, 146–157. <https://doi.org/10.1093/jpe/rtw094>

Google Scholar: [Author Only](#) [Title Only](#) [Author and Title](#)

Ter-Mikaelian, M.T., Parker, W.C., 2000. Estimating biomass of white spruce seedlings with vertical photo imagery. *New Forests* 20, 145–162. <https://doi.org/10.1023/A:1006716406751>

Google Scholar: [Author Only](#) [Title Only](#) [Author and Title](#)

Trogisch, S., Liu, X., Rutten, G., Xue, K., Bauhus, J., Brose, U., Bu, W., Cesarz, S., Chesters, D., Connolly, J., Cui, X., Eisenhauer, N., Guo, L., Haider, S., Härdtle, W., Kunz, M., Liu, L., Ma, Z., Neumann, S., Sang, W., Schuldt, A., Tang, Z., van Dam, N.M., von Oheimb, G., Wang, M.-Q., Wang, S., Weinhold, A., Wirth, C., Wubet, T., Xu, X., Yang, B., Zhang, N., Zhu, C.-D., Ma, K., Wang, Y., Bruelheide, H., 2021. The significance of tree-tree interactions for forest ecosystem functioning. *Basic and Applied Ecology, Tree Diversity Effects on Ecosystem Functioning* 55, 33–52. <https://doi.org/10.1016/j.baae.2021.02.003>

Google Scholar: [Author Only](#) [Title Only](#) [Author and Title](#)

Tyree, M.T., Ewers, F.W., 1991. The hydraulic architecture of trees and other woody plants. *New Phytologist* 119, 345–360. <https://doi.org/10.1111/j.1469-8137.1991.tb00035.x>

Google Scholar: [Author Only](#) [Title Only](#) [Author and Title](#)

Tyree, M.T., Sperry, J.S., 1989. Vulnerability of Xylem to Cavitation and Embolism. *Annual Review of Plant Physiology and Plant Molecular Biology* 40, 19–36. <https://doi.org/10.1146/annurev.pp.40.060189.000315>

Google Scholar: [Author Only](#) [Title Only](#) [Author and Title](#)

van Genuchten, M.Th., 1980. A Closed-form Equation for Predicting the Hydraulic Conductivity of Unsaturated Soils. *Soil Science Society of America Journal* 44, 892–898. <https://doi.org/10.2136/sssaj1980.03615995004400050002x>

Google Scholar: [Author Only](#) [Title Only](#) [Author and Title](#)

Vitali, V., Forrester, D.I., Bauhus, J., 2018. Know Your Neighbours: Drought Response of Norway Spruce, Silver Fir and Douglas Fir in Mixed Forests Depends on Species Identity and Diversity of Tree Neighbourhoods. *Ecosystems* 21, 1215–1229. <https://doi.org/10.1007/s10021-017-0214-0>

Google Scholar: [Author Only](#) [Title Only](#) [Author and Title](#)

Wambsganss, J., Beyer, F., Freschet, G.T., Scherer-Lorenzen, M., Bauhus, J., 2021. Tree species mixing reduces biomass but increases length of absorptive fine roots in European forests. *Journal of Ecology* 109, 2678–2691. <https://doi.org/10.1111/1365-2745.13675>

Google Scholar: [Author Only](#) [Title Only](#) [Author and Title](#)

Waxman, M.H., Smits, L.J.M., 1968. Electrical Conductivities in Oil-Bearing Shaly Sands. *Society of Petroleum Engineers Journal* 8, 107–122. <https://doi.org/10.2118/1863-A>

Google Scholar: [Author Only](#) [Title Only](#) [Author and Title](#)

Competing Interest Statement

Authors declare no competing interest.

ACCEPTED MANUSCRIPT